Two-parameter nonsmooth bifurcations of limit cycles: classification and open problems

P. Kowalczyk[*], M. di Bernardo[*†], A.R. Champneys[*], S.J. Hogan[*],
M. Homer[*], Yu.A. Kuznetsov[‡], A. Nordmark[§], P.T. Piiroinen[*]

February 10, 2005

Abstract

This paper proposes a strategy for the classification of codimension-two grazing bifurcations of limit cycles in piecewise smooth systems of ordinary differential equations. Such nonsmooth transitions (C-bifurcations) occur when the cycle interacts with a discontinuity boundary of phase space in a non-generic way. Several such codimension-one events have recently been identified, causing for example period-adding or sudden onset of chaos. Here, the focus is on codimension-two grazings that are local in the sense that the dynamics can be fully described by an appropriate Poincaré map from a neighbourhood of the grazing point (or points) of the critical cycle to itself. It is proposed that codimension-two grazing bifurcations can be divided into three distinct types: either the grazing point is degenerate, or the the grazing cycle is itself degenerate (e.g. non-hyperbolic) or we have the simultaneous occurrence of two grazing events. A careful distinction is drawn between their occurrence in systems with discontinuous states, discontinuous vector fields, or that have discontinuity in some derivative of the vector field. Examples of each kind of bifurcation are presented, mostly derived from mechanical applications. For each example, where possible, principal bifurcation curves characteristic to the codimension-two scenario are presented and general features of the dynamics discussed. Many avenues for future research are opened.

1 Introduction

A wide range of systems of relevance to science and engineering applications can be modelled by sets of ordinary differential equations (ODEs) of the form

$$\dot{x} = f(x), \qquad x \in \mathbb{R}^n, \tag{1}$$

featuring different types of discontinuous right-hand sides (RHS) $f(x)$ where x is the state vector (see for example[Brogliato 1999, Zhusubaliyev, et al. 2001, Leine 2000, di Bernardo, et al. 2004, di Bernardo, et al. 2005]). (Dependence of $f(x)$ on parameters $\mu \in \mathbb{R}^m$ is not indicated for simplicity). Examples in applications include, just to mention a few, power converters in electronic engineering [Banerjee & Verghese 2001, di Bernardo, et al. 1998], mechanical systems with impacts and/or friction [Brogliato 1999, Chin, et al. 1994, Dankowicz & Nordmark 1999, di Bernardo, et al. 2003b], walking robots [Brogliato 1999, Piiroinen 2002], hybrid and relay control systems [Kowalczyk & di Bernardo 2001b]. Recently, it has been shown that these systems can exhibit complex dynamics whose occurrence cannot be explained using bifurcation analysis tools developed for smooth dynamical systems. For example, one of the most striking feature of this class of systems is that they often exhibit sudden transitions from periodic

[*]Department of Engineering Mathematics, University of Bristol, University Walk, Bristol BS8 1TR, U.K
[†]also Dipartimento di Informatica e Sistematica, Universita degli Studi di Napoli, Naples, Italy
[‡]Mathematisch Instituut, Universiteit Utrecht, Budapestlaan 6, 3584 CD Utrech, The Netherlands
[§]School of Sciences, Mechanics, Royal Institute of Technology (KTH), Stockholm 100 44, Sweden

attractors to chaos in the absence of any period-doubling or other bifurcation cascade usually observed in their smooth counterparts. In fact, a new class of bifurcations, or *nonsmooth bifurcations*, needed to be introduced to explain these phenomena. As further detailed below, so-called border collision and grazing bifurcations were shown to be the main cause for such unexpected transitions which were left unexplained for a relatively long time in the nonlinear dynamics literature (see for example [Banerjee & Verghese 2001] for an account of the historical developments in the analysis of nonlinear phenomena in power electronic systems).

Most of the analysis of nonsmooth bifurcations has focused so far on those transitions that can be observed under variation of one of the system parameters. More precisely, codimension-one nonsmooth bifurcations were the subject of much research effort aimed at their classification and analytical characterisation. Despite the successes of nonsmooth bifurcation theory in explaining the complex behaviour observed, for instance, in power converters or mechanical systems with impacts and friction many open problems still remain. Among these, the strongest limitation of the existing theory of nonsmooth bifurcations is probably the ability to study phenomena that can be observed by varying just one parameter. In applications, systems are often characterised by many parameters of interest. Take, for example, a power electronic circuit. Here, the simplest possible circuit schematic will contain at least three components (a resistor, an inductance and a capacitor). Therefore, it is of utmost importance to be able to characterise the system bifurcation behaviour under variation of two or more parameters.

The main aim of this paper is to present a first attempt at classification of possible codimension-two nonsmooth bifurcations of limit cycles in impacting and piecewise-smooth flows. Rather than being an exhaustive review of available results, the aim is to offer a *preview* of a number of possible codimension-two events unique to nonsmooth systems which will be unfolded in details. In so doing, only hints will be given of the ensuing dynamics but for each chosen possibility, a representative system will be used as an example to illustrate the effects of the codimension-two bifurcation under investigation. Our hope is that this paper can act as a spur for future analyses of other codimension-two degeneracies and for other to use as a guide for understanding dynamics in nonsmooth applications. The paper provides the foundations of a rational classification of two-parameter nonsmooth bifurcations of limit cycles in flows based on their codimension. It is worth emphasising here that most of the novel codimension-two bifurcations described in the paper are presented here for the first time.

The rest of the paper is outlined as follows. In Sec. 3, after a brief resumé of codimension-one grazing bifurcations and their non-degeneracy conditions, a broad classification of codimension-two C-bifurcations into three different types is proposed. In the three sections that follow examples of each type are presented. Sec. 4 treats codimension-two C-bifurcations that fail a non-degeneracy condition at the grazing point, using sliding bifurcations in a dry friction oscillator as an physical example. Sec. 5 treats C-bifurcations where the linearisation around the non-grazing limit cycle is degenerate, again using a dry-friction example in the sliding case, but also an example of an impacting system where there is grazing of a non-hyperbolic orbits. The third type of codimension-two C-bifurcations, where two independent grazing events occur along a cycle, is discussed in Sec. 6, again looking at a specific example in a sliding system. Finally, in Sec. 7 conclusions and open problems are discussed.

2 Systems of interest

Here, as in [di Bernardo et al. 2004, di Bernardo et al. 2005], we will assume that the discontinuities occur across finitely many manifolds in phase space, called *discontinuity* or *switching* sets. Following [Leine 2000], we divide the nonsmooth dynamical systems of interest into three different categories, depending on the discontinuity type of their orbits and vector fields f:

Class A. Systems with discontinuous orbits, or *impacting systems*. These are represented by ODEs with Dirac δ discontinuities in the RHS function f, for example impacting systems

or vibro-impacting machines [Brogliato 1999, Pavlovskaia & Wiercigroch 2003]. Such systems are more commonly formulated without using delta-functions, as a *hybrid system* [Van der Schaft & Schumacher 2000] with the discontinuous jumps (such as a restitution law) described by auxiliary maps.

Class B. Systems with continuous but not continuously differentiable orbits, that is, *Filippov systems* [Filippov 1988] with discontinuous f. Such systems arise as models of power-electronics voltage converters [di Bernardo et al. 1998, Fossas & Olivar 1996], and dry-friction oscillators [Galvanetto 1997, Popp & Shelter 1990] and relay-controlled ecosystems [Dercole, et al. 2003]. Such systems often feature so called *sliding motion*, that is constrained to move within a discontinuity set.

Class C. Nonsmooth systems whose orbits and vector fields are everywhere *continuous*, or *piecewise smooth continuous systems*. Such systems have continuously-differentiable orbits but discontinuities in the first or higher derivatives of f. Examples include mechanical systems with bi-linear elastic support [Shaw & Holmes 1983, Thompson, et al. 1983]

Sometimes systems from classes **B** and **C** together are called piecewise-smooth (PWS) flows. We write such systems as

$$\dot{x} = F_i(x), \qquad x \in G_i, \tag{2}$$

where $G_i,\ i = 1, 2, \ldots, N$, are finitely many open domains of an n-dimensional state space (phase space) which is a differentiable manifold. The $(n-1)$-dimensional boundaries between G_i and G_j are labelled as Σ_{ij} for $i < j$. We assume that these *discontinuity sets* are smooth, that is they can be defined by

$$\Sigma_{ij} = \{H_{ij}(x) = 0\},$$

where H_{ij} is a smooth function from $\mathbb{R}^n$ to $\mathbb{R}$. For example, when only one smooth discontinuity set is present

$$\Sigma = \Sigma_{12} = \{H(x) = 0\} \tag{3}$$

(2) can be written in the form

$$\dot{x} = \begin{cases} F_1(x), & H(x) > 0, \\ F_2(x), & H(x) < 0 \end{cases} \tag{4}$$

For a system with discontinuous orbits (class **A**), several formalisms are available. For example, we can write a differential equation (1) with δ-function discontinuities in the RHS. Such an equation is more properly regarded as a *measure differential inclusion* [Aubin & Cellina 1984]. Alternatively, we can use the terminology of *complementarity systems* [Brogliato 1999] which are inspired by mechanical systems with inequality constraints. Perhaps the most natural way to study them though is as a specific form of *hybrid systems*, where a set of smooth differential equations (4) is augmented with *reset maps* of the form

$$R_{ij,kl} : \Sigma_{ij} \to \Sigma_{kl}, \quad x^+ = g_{ij,kl}(x^-).$$

Near a single discontinuity boundary, we shall assume the following simplified form [di Bernardo et al. 2004]

$$\dot{x} = F(x) \quad \text{if } H(x) > 0 \tag{5}$$

with impact at the surface defined by $H(x) = 0$, and where the impact law takes the form

$$x^+ = R(x^-) = x^- + G(x^-)H_x F(x^-). \tag{6}$$

with G being a smooth function. Note that more complicated forms of the reset map are possible: for example in systems modelling impact with friction, e.g. [Stewart 2000]. For convenience, we will also define the velocity and acceleration (of the vector field F relative to H)

$$v(x) = H_x F(x)$$
$$a(x) = (H_x F)_x F(x).$$

2.1 Codimension-one nonsmooth bifurcations

Apart from standard bifurcations (fold, Hopf etc.), systems from all three of the classes presented in the previous section can undergo topological changes to their phase portraits that are unique to nonsmooth systems. For example, as a parameter is varied, an equilibrium point in G_i can approach a boundary Σ_{ij}. Many possibilities can emerge from such a nonsmooth bifurcation point. For example, Hopf-like bifurcations can occur, generating limit cycles from the boundary equilibrium, but with a linear rather than square-root growth in amplitude [Bautin & Leontovich 1976, Filippov 1988, Gubar' 1971, Kunze 2000, Kuznetsov, et al. 2002]. There are also nonsmooth analogues of folds [Leine 2000]. Limit cycles of discontinuous systems can also exhibit other novel nonsmooth transitions as elucidated in the the pioneering work in the Russian and Czech literature, such as that of Feigin [Fedosenko & Feigin 1972, Feigin 1970, Feigin 1974, Feigin 1978, Feigin 1995, Feigin 1994] and Peterka [Peterka 1974a, Peterka 1974b, Peterka 1992]. In Feigin's work, all scenarios involving invariant sets undergoing a non-structurally stable interaction with a discontinuity set were given the collective name of *C-bifurcations* (C stands for the Russian word for 'sewing'). As remarked in [di Bernardo, et al. 2003a], however, such a definition does not necessarily imply a bifurcation in the strict mathematical sense of transition to a topologically non-equivalent phase portrait (see, e.g. [Kuznetsov 2004]), because the existence and stability of invariant sets can be unaffected by such an interaction (especially for systems of class **C**). So, it might be more correct to refer to such discontinuity-set driven events as *nonsmooth transitions* rather than bifurcations in the classical sense.

Bifurcations of fixed points in PWS discrete-time maps were more recently studied in the West by Yorke and collaborators [Nusse & Yorke 1992, Nusse, et al. 1994, Yuan, et al. 1998]. Interactions of periodic points with the discontinuity set in continuous piecewise-linear (PWL) maps were termed *border-collision bifurcations*. It was later shown in [di Bernardo, et al. 1999] that border-collision bifurcations may be interpreted in terms of Feigin's theory. Thus, they lead to a number of bifurcation scenarios (saddle-node like cases, period doublings, transcritical-like transitions), which can be classified in $n-$dimensional cases by applying a set of appropriate conditions on the eigenvalues of the linear part of a PWS map on either side of the discontinuity.

Another important class of C-bifurcations are so-called *grazing bifurcation*, when a limit cycle undergoes either a tangential interaction with a discontinuity set, or passes through the intersection between two discontinuity sets. It is these nonsmooth transitions that form the subject of this paper. To analyse and classify the dynamics that can ensue from such limit cycle transitions, an established technique is to derive PWS maps as 'normal forms' for the bifurcation. Iterates of the derived maps then give the existence of nearby invariant sets. The derivation of such maps is based on the concept of the *zero time discontinuity mapping* (ZDM) introduced by Nordmark [Nordmark 1991]. These normal forms were derived for all three classes of nonsmooth dynamical systems mentioned above [Nordmark 1991, Fredriksson & Nordmark 2000, di Bernardo, et al. 2001b, di Bernardo, et al. 2001a, Kowalczyk & di Bernardo 2004]. Interestingly, in none of the cases, other than a boundary-intersection crossing in a class **B** system [di Bernardo et al. 2001b] does this lead to a locally piecewise-linear map of the kind studied by Feigin or Yorke. Instead, depending on the local properties of the vector fields across the discontinuity, tangential grazing in the absence sliding leads to a ZDM with an $O(k+1/2)$ term, for some non-negative integer k [di Bernardo et al. 2001a, Fredriksson & Nordmark 2000]. In contrast, boundary intersection in the absence of sliding leads to maps with a discontinuity of one order less than that of the vector field. There are more possibilities of grazing bifurcations in vector fields in which sliding occurs, as we shall see in the next section. In general these all lead to maps with jumps in derivatives of higher than linear order, except for the so-called *grazing-sliding* case. This case, which occurs in models of dry-friction oscillators [Wiercigroch & de Kraker 2000] and relay controllers [Kowalczyk & di Bernardo 2001b], leads to a piecewise-linear normal form map. However, this map is not of the form used by Feigin or Yorke, because it is non-invertible on one side of the discontinuity. Such non-invertibility has significant implications regarding

possible bifurcation scenarios that can be observed (see [Parui & Banerjee 2002, Kowalczyk 2005] for further details).

So far, the investigation of nonsmooth bifurcations has focused on one-parameter transitions. Here, we should comment on the notion of the *codimension* of C-bifurcations. Assuming the weak definition as non-generic interaction with a discontinuity set, we propose to use a utilitarian definition of the codimension of a bifurcation completely analogous to the one used for smooth systems – see e.g [Kuznetsov 2004]. Namely, the codimension of a bifurcation is defined as the difference between the dimension of the parameter space and the corresponding set of parameters for which the bifurcation occurs.

Recent theory has provided unfoldings of several different kinds of codimension-one C-bifurcations of limit cycles in piecewise-smooth systems. The following subsections itemise the cases that have so far been analysed. We give only the scantiest details but provide references where the interested reader may find out more. It might also be useful to point out that there are other cases of more global bifurcations that have been treated in full for planar systems [Kuznetsov et al. 2002] and of various ad hoc analyses in special cases, e.g. [Zhusubaliyev & Mosekilde 2003].

2.1.1 Tangential grazing in PWSC systems (Class C)

Grazing in piecewise smooth continuous systems (class **C**) have been analysed in some generality by Dankowicz & Nordmark [Dankowicz & Nordmark 1999] and by di Bernardo, Budd and Champneys [di Bernardo et al. 2001a]. Here we present results only for the special case of so-called *uniform* discontinuity of degree m across the discontinuity boundary Σ at which grazing occurs. That is one can write

$$F_2(x) = F_1(x) + W(x)H(x)^{m-1}. \tag{7}$$

for some smooth function W. Then the following result holds:

Theorem 2.1 ([Nordmark 2002]) *Suppose a hyperbolic periodic orbit grazes quadratically from the C_1 side at $x = x^*$ with a discontinuity boundary Σ (3) in a PWS system (4) with discontinuity of type (7) for $m \geq 2$. That is*

$$H(x^*) = 0, \qquad H_x F_1(x^*) = 0, \qquad (H_x F_1)_x F_1(x^*) > 0, \tag{8}$$

the ZDM is given by

$$x \mapsto \begin{cases} x & \text{if} \quad H_{\min}(x) \geq 0 \\ x + \mathrm{e}(x,y)y^{2m-1} & \text{if} \quad H_{\min}(x) \leq 0 \end{cases} \tag{9}$$

where $y = \sqrt{-H_{\min}(x)}$ and $H_{\min}(x)$ is the local minimum value of $H(x)$ attained along an orbit flowing under F_1. here, e *is a smooth function whose lowest order term is*

$$\mathrm{e}(x,0) = 2(-1)^{m+1} I(m) W(x) \sqrt{\frac{2}{(H_x F_1)_x F_1(x)}},$$

with

$$I(m) = \int_0^1 (1-\xi^2)^{m-1} d\xi; \qquad I(2) = \frac{2}{3}, \quad I(3) = \frac{8}{15}, \quad I(4) = \frac{16}{35}, \ldots.$$

Let P be the Poincaré map associated with the periodic orbit, ignoring any local touching of Σ. The dynamics of the composite map $P \circ ZDM$ can be unfolded by adding parameters in a generic way. Note that since the singularity of the map (9) is of order $x^{3/2}$ or higher to leading order, then there is no immediate bifurcation of the simplest fixed point of the map corresponding to the periodic orbit. However, in applications this singularity can cause a local bifurcation, such as a catastrophic fold or period doubling cascade, leading to chaos to occur for very nearby parameter values [Dankowicz & Nordmark 1999]. Note the non-degeneracy condition in (8) which guarantees that the grazing bifurcation is of codimension-one.

2.1.2 Tangential grazing in impacting systems (Class A)

As with class **C** systems, we can formulate defining and non-degeneracy conditions for a point x_0, assumed to part of a limit cycle to be a grazing point. We demand that

$$\begin{aligned} H(x_0) &= 0 && (10)\\ H_x F(x_0) &= 0 && (11)\\ (H_x F)_x F(x_0) &> a_0 > 0 && (12) \end{aligned}$$

Theorem 2.2 (Nordmark's ZDM for grazing impact [di Bernardo et al. 2004]) *Given the non-degeneracy conditions* (10)*,* (11) *and* (12)*, then close to* x_0 *the ZDM can be written as*

$$ZDM(x) = x + \begin{cases} 0 & \text{if } H_{\min}(x,v) \geq 0 \\ \beta(x,y,v)y & \text{if } H_{\min}(x,v) < 0 \end{cases} \tag{13}$$

where

$$\begin{aligned} \beta(x,y,v) &= -G(x)\sqrt{2a} + r_2(x,y,v)\\ r_2(x,y,v) &\to 0 \quad \text{if } y,v \to 0\\ y(x,v) &= \sqrt{-H_{\min}(x,v)}\\ H_{\min}(x,v) &= H(x) - v^2\left(\frac{1}{2a} + r_1(x,v)\right)\\ r_1(x,v) &\to 0 \quad \text{if } v \to 0\\ v(x) &= H_x F(x)\\ a(x) &= v_x F(x), \end{aligned} \tag{14}$$

and $r_{1,2}$ *are smooth in their arguments.*

Hence the local change to the Poincaré map close to grazing has a square root singularity. Depending on the Floquet multipliers of the periodic orbit prior to grazing, this can lead to the sudden onset of chaotic attractors with a characteristic fingered structure, or to a sequence of period-adding bifurcations. The interested reader is referred to [Chin et al. 1994, Nordmark 2002, Budd & Dux 1994], for example, for more details of these intricate dynamical possibilities.

2.1.3 Sliding bifurcations in Filippov systems (class B)

Sliding occurs when the vector fields F_1 and F_2 point toward Σ from both sides of the manifold. The sliding region of Σ is denoted by $\hat{\Sigma}$ in Fig. 1 and what follows. Whilst sliding, the flow can be shown to correspond to an effective vector field F_s given by [Filippov 1988, Utkin 1992]

$$F_s = \frac{F_1 + F_2}{2} + \frac{F_2 - F_1}{2}\beta(x) \tag{15}$$

where

$$\beta(x) = -\frac{H_x(F_1 + F_2)}{H_x(F_2 - F_1)} \in [-1,\ 1]. \tag{16}$$

We define the sliding region as

$$\hat{\Sigma} := \{x \in \Sigma : |\beta(x)| \leq 1\} \tag{17}$$

and its boundaries as

$$\partial\hat{\Sigma}^{\pm} := \{x \in \Sigma : \beta(x) = \pm 1\}. \tag{18}$$

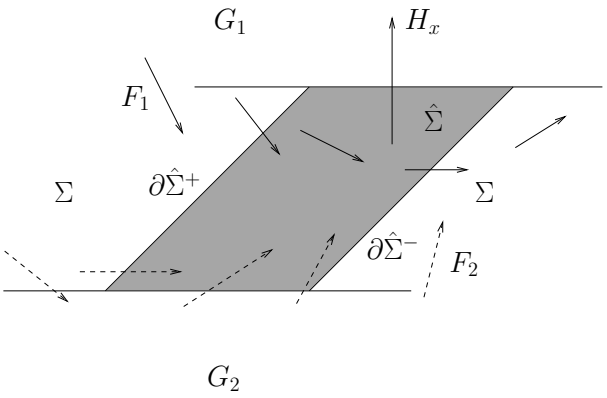

Figure 1: Schematic illustration of the vector fields F_1 and F_2 close to a sliding portion of a discontinuity boundary Σ in a class **B** system.

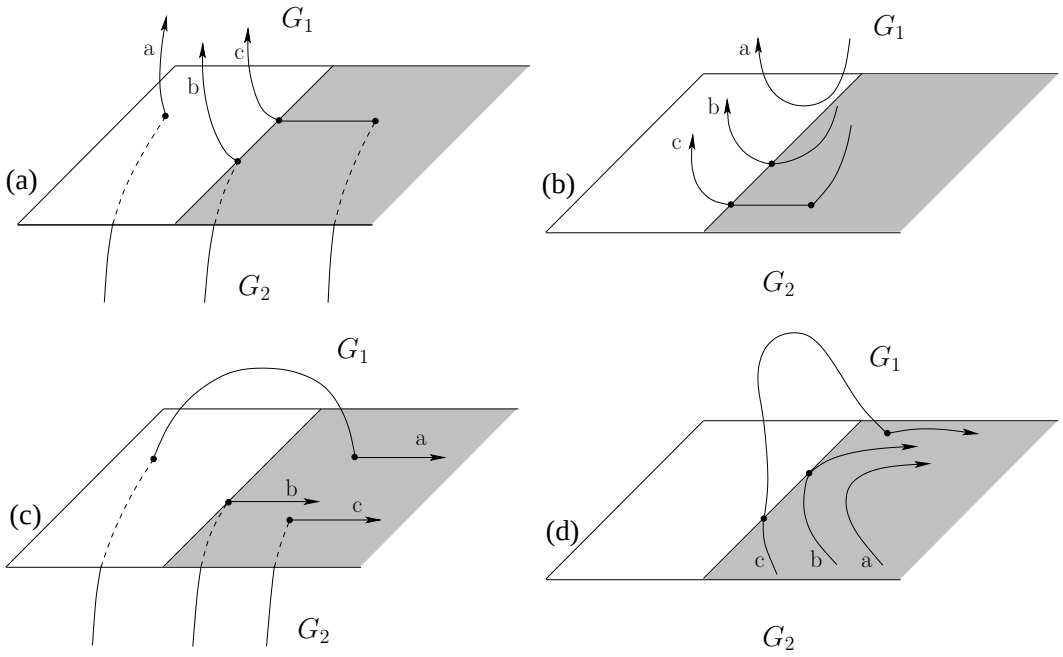

Figure 2: codimension-one sliding bifurcations of limit cycles in a class **B** system.

Bifurcations	ZDM leading order term
crossing-sliding	$\varepsilon^2 + \mathcal{O}(\varepsilon^3)$
grazing-sliding	$\varepsilon + \mathcal{O}(\varepsilon^{3/2})$
switching-sliding	$\varepsilon^3 + \mathcal{O}(\varepsilon^4)$
adding-sliding	$\varepsilon^2 + \mathcal{O}(\varepsilon^{5/2})$

Table 1: Leading order terms of the zero-time discontinuity mappings for sliding bifurcations.

In the following we only consider the case when the sliding region is attracting; that is when

$$H_x(F_2 - F_1) > 0, \tag{19}$$

(although repelling sliding can arise as a consequence of the bifurcations we consider).

Sliding bifurcations are defined as tangential interactions between a limit cycle and the boundary of the sliding region $\partial\hat{\Sigma}$. Four distinct cases have been identified [Feigin 1994, Kowalczyk & di Bernardo 2001b, Kowalczyk & di Bernardo 2001a], see Fig. 2. Here one should interpret the three orbit segments a, b and c as belonging to a limit cycle at different parameter values. Following the now generally agreed nomenclature [di Bernardo et al. 2004], the scenario in Fig. 2(a) is called a *crossing-sliding bifurcation*, the case in panel (b) is called a *grazing-sliding bifurcation*, that in panel (c) a *switching-sliding bifurcation*, and that in (d) an *adding-sliding bifurcation*. See [di Bernardo, et al. 2002, di Bernardo et al. 2003b], for an unfolding of the dynamics that must ensue close to each such singularity. Table 1 summarises information on the leading-order term in the ZDM, i.e. the jump that ensues in the appropriate Poincaré map that unfolds the bifurcation.

It will be instructive for what follows to delineate the non-degeneracy hypotheses that underly the geometry in Fig. 2. We focus here only on the crossing-sliding case in panel (a). To be definite, using the notation from Fig. 1, we consider bifurcations with respect to the boundary $\partial\hat{\Sigma}^-$, so that the outgoing flow is generated by the vector fields F_1 or F_s but the incoming one might be generated by any of the three vector fields F_1, F_2 or F_s depending on the bifurcation scenario. Also, note from the orbit labelled b in Fig. 2(a) and (b), that the outgoing flows behave in a qualitatively equivalent way. Thus, the same set of analytical conditions defines these two sliding bifurcation scenarios. To make a distinction between them, knowledge of the incoming flows is also required.

Defining equations for the two bifurcations in question can be expressed by the following conditions evaluated precisely at the grazing point:

$$H(x) = 0, \quad H_x \neq 0, \tag{20}$$

$$\left.\frac{d(H(\Phi_1(x,t)))}{dt}\right|_{t=0} = H_x F_1 = 0. \tag{21}$$

where Φ_i represents the flow corresponding to vector field F_i; for ease of presentation we assume that Σ is locally flat, that is $\{H = 0\}$ is a hyperplane. To this we must add *non-degeneracy conditions*. For crossing-sliding we require an additional condition to ensure that after grazing, the orbit does indeed leave Σ:

$$\left.\frac{d(\beta(\Phi_1(x,t)))}{dt}\right|_{t=0} = \beta_x F_1 < 0. \tag{22}$$

where β_x is given by

$$\beta_x = -2\frac{H_x F_{1x}}{H_x F_2}. \tag{23}$$

is a vector normal to normal to $\partial\hat{\Sigma}^-$ within Σ. Note that (22) is really a non-degeneracy condition, because positive β_x makes no sense in this context; we should interpret this as saying

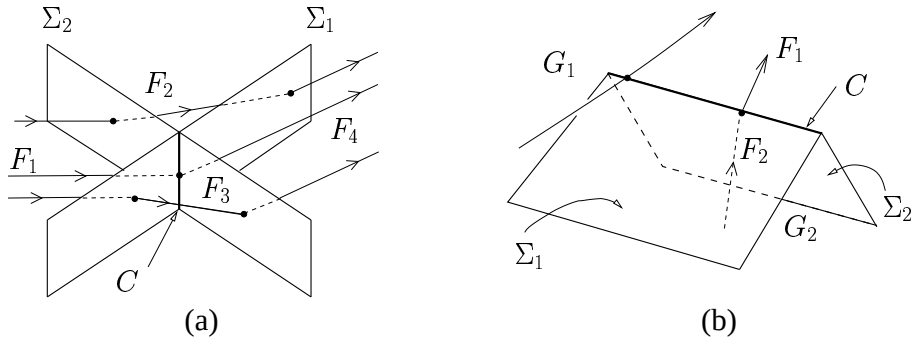

Figure 3: Schematics illustrating the (a) correspondence between an orbit that crosses the intersection between two discontinuity sets, and (b) in the case where $F_1 = F_3 = F_4$ found in DC/DC power converters

that no extra tangency occurs that would be quantified by a zero of β_x. After substituting for β_x and noting that $H_x F_2 > 0$ on $\partial\hat{\Sigma}^-$, (see eq. (19)) we can write condition (22) above as

$$\left.\frac{d^2(H(\Phi_1(x,t)))}{dt^2}\right|_{t=0} = H_x F_{1x} F_1 > 0. \tag{24}$$

2.1.4 Boundary-intersection crossing bifurcations

Another codimension-one case that will concern us in what follows is when two discontinuity surfaces cross as in Fig. 3(a). Then again, it will generically be a codimension-one phenomenon for a limit cycle to cross such an $(n-2)$-dimensional boundary-intersection surface. Motivated by examples in power electronics where a power source is switched on or off by comparing an output with a saw-tooth signal [di Bernardo et al. 2001b, Banerjee & Verghese 2001, Fossas & Olivar 1996], we shall in what follows consider the simpler situation where three of the vector fields at such a point are identical. Then we can consider the boundary intersection as a single nonsmooth discontinuity, i.e. having a *corner* [di Bernardo et al. 2001b] (see Fig. 3(b)). In the neighbourhood of such an effective discontinuity in the discontinuity set it is convenient to write $\Sigma_{12} = \Sigma_1 \cup \Sigma_2$, where

$$\Sigma_1 = \{H_1(x) = 0,\ H_2(x) \leq 0\}, \qquad \Sigma_2 = \{H_2(x) = 0,\ H_1(x) \leq 0\}, \tag{25}$$

where each of the $H_{1,2}$ are smooth functions.

Suppose we have a class **B** system. The simplest case is that we have no sliding in the vicinity of the corner-colliding limit cycle. Such a case was analysed in [di Bernardo et al. 2001b]. Taking the form of discontinuity sets Σ_1 and Σ_2 given by (25), non-degeneracy hypotheses can be formulated in terms of the angles between F_i and H_i. Specifically we assume (without loss of generality, up to a reversal of time if necessary)

$$H_{1x} F_i > 0, \quad H_{2x} F_i > 0, \quad \text{for} \quad i = 1, 2. \tag{26}$$

Note that there are two kinds of orbit that can satisfy these constraints, which we refer to as an *external* or *internal* corner collision, see Fig. 4.

We consider external corner-collision; the internal case is analysed in an entirely analogous manner [di Bernardo et al. 2001b]. Then it can be shown that the ZDM for an orbit that crosses the wedge, when solving for the flow as if the vector field F_1 applied everywhere, is given by

$$x \mapsto \begin{cases} x & \text{if non-crossing,} \\ x + (F_1^0 - F_2^0) a_2 x + o(|x|) & \text{if crossing,} \end{cases} \tag{27}$$

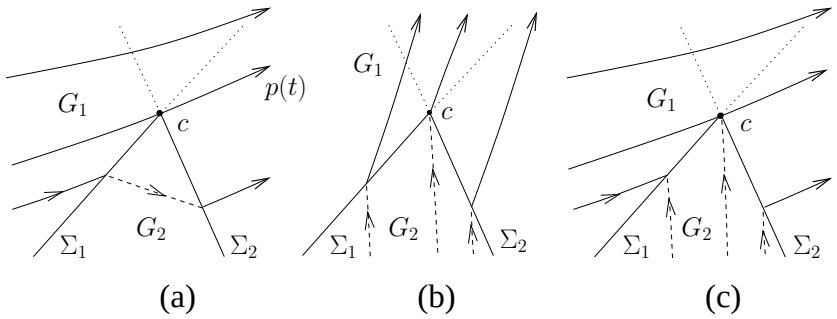

Figure 4: Schematic, in a general two-dimensional slice, of orbits in the neighbourhood of the three types of interaction with the corner depicted in Fig. 3(b): (a) external corner-collision; (b) internal; and (c) which does not satisfy the hypotheses (26)

where

$$a_2 = J_2 - J_2 F_1^0 J_1, \qquad J_i = \frac{H_{ix}^0}{H_{ix}^0 F_i^0}\,. \tag{28}$$

which gives a piecewise-linear map when composed with the smooth Poincaré map around the corner-colliding periodic orbit. Note that similar arguments show that if the vector field were continuous, but with discontinuous nth derivative, then one should generically expect a map with a jump in the $(n+1)$st derivative.

3 Proposed classification of codimension-two C-bifurcations

The classification approach proposed here is similar to the one used to classify codimension-two bifurcations in smooth systems. Generically, smooth codimension-two bifurcations are encountered when [Guckenheimer & Holmes 1983, Wiggins 1990, Kuznetsov 2004]:

(1) standard codimension-one bifurcations (e.g. a saddle-node cycle), with an additional degeneracy in the nonlinear terms of the normal form (e.g. a cusp of cycles);

(2) the linear part of the vector field or the associated Poincaré map at the bifurcation event is doubly degenerate, e.g. quasiperiodic instability with strong resonances;

(3) a global and a local event occur simultaneously, e.g. a Shilnikov-Hopf bifurcation, a homoclinic orbit to a resonant saddle, or a non-central homoclinic orbit to a saddle-node;

(4) two global bifurcations happen at once, e.g. the appearance of two homoclinic orbits to a saddle or two heteroclinic orbits connecting two saddles ("a heteroclinic contour").

We shall now use a similar approach to that for smooth bifurcations outlined above to classify the different ways that these bifurcations may become degenerate, while remaining local in the sense that they can be unfolded in terms of Poincaré maps defined in a neighbourhood of the grazing point(s). Thus, we propose that codimension-two C-bifurcations for limit cycles can be put into one of the following three types:

Type I: **Degenerate grazing point**; that is, there is a degeneracy of one of the analytical conditions determining the properties of the vector fields local to the grazing event. This is analogous to degenerate normal form coefficients for smooth bifurcations. This is likely to influence the leading order term of the normal form map derived via the discontinuity mapping.

Type II: **C-bifurcations of degenerate cycles**, i.e. bifurcations where the linear part of the Poincaré map around the orbit contains a degeneracy. The most obvious case, and the one we shall focus on in this paper is that the critical cycle is non-hyperbolic. Note however that to determine hyperbolicity of the critical cycle might be non-trivial. For instance, the critical cycle undergoing a grazing-sliding bifurcation can be viewed as a cycle with and without the zero-length sliding segment. In the former case its stability and hence its hyperbolicity can be determined by solving variational equations. In the later we need to solve variational equations together with the ZDM techniques.

This type can be also seen as a combination of a smooth and a nonsmooth bifurcation occurring at the same parameter value.

Type III: **Simultaneous occurrence of two grazings** at two different points along the critical orbit. The possibilities here are large. Each of the bifurcations outlined in the previous section could occur along lines in a parameter plane. Independently, at another point along the critical periodic orbit, a second grazing event could occur. This would then form the intersection point in two-parameter space between these two lines of independent codimension-one bifurcations. However, in an unfolding one might well find that other bifurcation curves necessarily emerge from such a codimension-two point.

In this paper we do not consider global bifurcations other than in the sense that the interaction between the discontinuity boundary and a limit cycle can be viewed in some sense as a global bifurcation involving a distinguished point on a limit cycle (analogously to homoclinic orbits). We make further comments about such possibilities in Sec. 7. In what follows, we shall further illustrate possibilities for each of the types highlighted above, drawing on representative examples and their numerical unfolding.

4 Type I: Degenerate grazing point

Let us start our considerations with Type I codimension-two C-bifurcations. We choose to consider sliding bifurcations of limit cycles accompanied by the violation of one of the analytical conditions which determine standard codimension-one sliding bifurcations. Therefore, we focus on codimension-two C-bifurcations falling into the category classified as Type I.

4.1 Degenerate sliding bifurcations

We begin by discussing in more detail when degenerate sliding bifurcations can be encountered. They occur when the vector field generating an incoming or an outgoing flow takes a non-generic position with respect to the boundary of the sliding region. In what follows the degenerate sliding-bifurcations will refer to codimension-two sliding bifurcations characterised by degeneracy of the outgoing flow only.

4.1.1 Degenerate crossing-sliding bifurcation

Suppose that a Filippov system (class **B**) exhibits a crossing-sliding bifurcation scenario. Let us assume that an additional continuous parameter variation makes the outgoing flow degenerate. Degeneracy of the vector field generating the outgoing flow Φ_1 can be viewed as an additional tangency of F_1 to the manifold

$$\Theta = \{\beta(x) = -1\}$$

crossing Σ along $\partial\hat{\Sigma}^-$ (see Fig. 5(b)). Depending on the behaviour of the vector field F_1 at the point of interaction with $\partial\hat{\Sigma}^-$, the outgoing flow might leave the switching manifold or evolve within the discontinuity set. We assume that at the contact with the boundary of the sliding region the orbit leaves Σ.

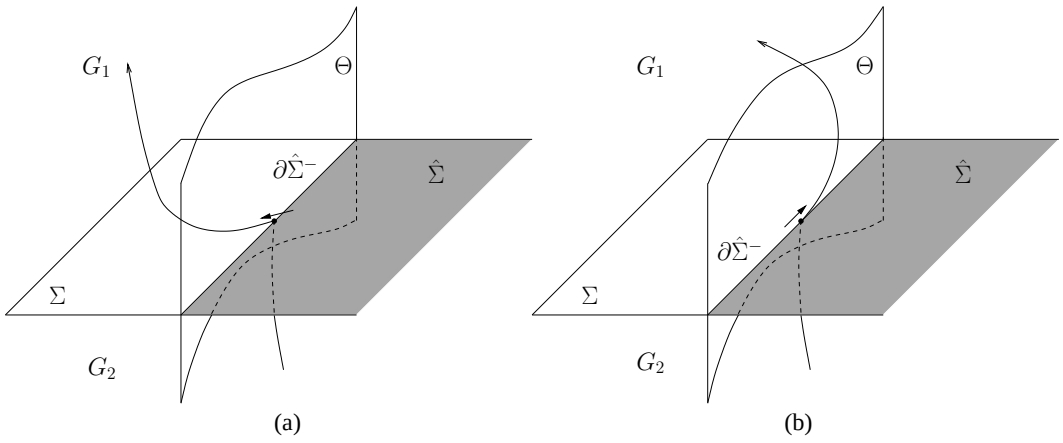

Figure 5: Critical orbit and the vector field generating the outgoing flow in (a) the crossing-sliding and (b) the degenerate crossing-sliding cases. Short arrows illustrate the behaviour of the vector field F_1 at the bifurcation point.

Information on the geometric properties of the vector field F_1 when interacting with $\partial\hat{\Sigma}^-$ allows us to formulate a set of analytical conditions that must be satisfied by F_1 at the codimension-two bifurcation point.

The degeneracy in the position of the vector field with respect to $\partial\hat{\Sigma}^-$ is expressed by the condition

$$\left.\frac{d(\beta(\Phi_1(x,t)))}{dt}\right|_{t=0} = \beta_x F_1 = 0. \tag{29}$$

Expressing condition (29) in terms of H_x and F_1 yields

$$\left.\frac{d^2(H(\Phi_1(x,t)))}{dt^2}\right|_{t=0} = H_x F_{1x} F_1 = 0. \tag{30}$$

Since we require the orbit to leave the switching manifold, the vector field F_1 should exhibit a local maximum with respect to $\partial\hat{\Sigma}^-$. Thus the non-degeneracy condition can be written as

$$\left.\frac{d^2(\beta(\Phi_1(x,t)))}{dt^2}\right|_{t=0} = \beta_x F_{1x} F_1 < 0. \tag{31}$$

Expressing (31) in terms of H_x, F_1 gives

$$\left.\frac{d^3(\beta(\Phi_1(x,t)))}{dt^3}\right|_{t=0} = H_x (F_{1x})^2 F_1 > 0. \tag{32}$$

A critical orbit in the case of codimension-one crossing-sliding bifurcation can be compared with the critical orbit when the crossing-sliding is degenerate (see Fig. 5(a) and (b) respectively).

A full unfolding of this codimension-two scenario is contained in [Kowalczyk & di Bernardo 2004]. There it can be shown that three independent codimension-one sliding bifurcations emanate from the codimension-two point. These are standard crossing-sliding, switching-sliding and grazing-sliding; see Fig. 6 for a graphical explanation. That all three must occur can be seen from the character of the vector field generating the outgoing flow, and by considering small perturbations applied to the system. Certain perturbations will cause a limit cycle to interact with the boundary of the sliding region with the vector field F_1, that no longer exhibits a maximum with respect to $\partial\hat{\Sigma}^-$. The vector field will either point out of, or into, the sliding region. Thus we should observe either the crossing or the switching-sliding scenario –

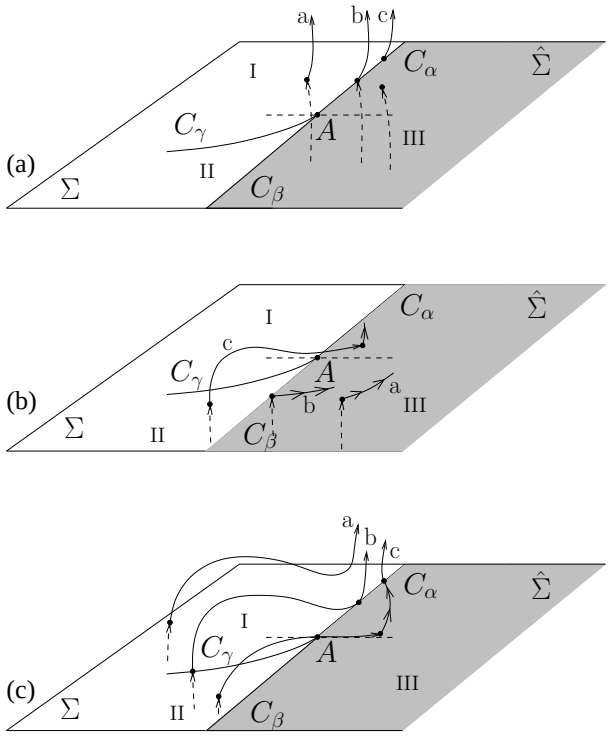

Figure 6: Codimension-one sliding bifurcations unfolded from the degenerate crossing-sliding of codimension-two. (a) crossing-sliding, (b) switching-sliding and (c) grazing-sliding bifurcation scenario.

see Fig. 6(a) and (b). In Fig. 6, C_α and C_β denote the boundaries of the sliding region and correspond to the crossing-sliding and switching-sliding boundaries in phase space. A denotes a point on $\partial\hat{\Sigma}^-$ where the vector field F_1 exhibits a local maximum. Lower case letters a, b and c denote segments of orbits forming parts of a limit cycle "before", "at" and "after" the bifurcation. By I, II and III we denote regions on Σ around A such that orbits rooted in each region differ by the number of different segments forming an orbit before a particular orbit leaves the neighbourhood of A. Note that the orbit starting in I, locally to A, has only a segment generated by the vector field F_1. The orbit rooted in region III has two segments locally to A – one formed by the vector field F_s another by F_1. Finally, the orbit rooted in region II features three segments locally to A – first generated by F_1 then by F_s and the third segment generated again by F_1. The crossing-sliding and switching sliding of codimension-one take into account transitions between orbits rooted in regions $I - II$ and $III - II$ correspondingly. Note that around A there is also possible transition between orbits rooted in regions I and III under the variation of one parameter. Such a transition would correspond to the grazing-sliding scenario as depicted in Fig. 6(c), but does not lead to any immediate topological change in the limit cycle since the ZDM of such a C-bifurcation is differentiable.

4.1.2 Other cases of degenerate sliding bifurcations of codimension-two

Different instances of degenerate sliding bifurcations can also occur. In fact, a straightforward analysis (presented in detail in [Kowalczyk & di Bernardo 2004]) shows what other codimension-one curves of sliding bifurcations must necessarily emanate from each such degenerate point. These results are summarised in Table 2. Here the defining conditions listed are just those that must be satisfied in addition to the usual ones defining the codimension-one singularity in question. Note the apparent discrepancy that the degenerate adding-sliding bifurcation scenario

Degenerate sliding bifurcation	Defining & non-degeneracy conditions	Other codim 1 bifurcations in unfolding
crossing-sliding	$H_x F_{1x} F_1 = 0$ $H_x (F_{1x})^2 F_1 > 0$	crossing-sliding switching-sliding grazing-sliding
grazing-sliding	$H_x F_{1x} F_1 = 0$ $H_x (F_{1x})^2 F_1 < 0$	grazing-sliding, adding-sliding
switching-sliding	same as above but incoming flow generated by F_2	switching-sliding, crossing-sliding, adding-sliding
adding-sliding	same as above but also $H_x (F_{1x})^2 F_1 = 0$ $H_x F_{1x} F_{1xx} F_1 F_1 + H_x (F_{1x})^3 F_1 < 0$	adding-sliding grazing-sliding

Table 2: Analytical conditions determining other three cases of degenerate codimension-two sliding bifurcations.

is characterised by *two*, not one, additional defining conditions. However, it can be argued that this is still a codimension-two event. The argument proceeds by considering the fact that the flow which interacts with the boundary of the sliding region is confined to evolution on the $n-1$ dimensional switching manifold Σ. In some sense, this loss of system dimension is reflected in the number of conditions determining the bifurcation and also in the number of non-degeneracy conditions that must be assumed. Further details of this subtle point are to be found in [Kowalczyk & di Bernardo 2004].

4.1.3 Example 1: Degenerate crossing-sliding in a forced linear dry-friction oscillator

We shall now give an example of a system where the degenerate crossing-sliding bifurcation scenario has been detected. In what follows we discuss the characteristic features of this C-bifurcation. In particular, we will focus on the parameter portrait around the codimension-two point.

Let us consider a dry-friction oscillator with external forcing, which can be expressed in non-dimensionalised form as:

$$\ddot{x} + x = \sin(\omega t) - F\mathrm{sgn}(\dot{x}), \tag{33}$$

where x is the position and $\dot{x}$ the velocity of the oscillating mass, while ω is the frequency of the forcing term and F is the amplitude of the dry friction. We can express equation (33) as a set of first order autonomous ODEs on the cylinder. After setting the variables $x_1 = x$, $x_2 = \dot{x}$ and $x_3 = \omega t (\mathrm{mod} 2\pi)$, (33) becomes:

$$\dot{x} = \begin{pmatrix} x_2 \\ -x_1 + \sin(x_3) - F\mathrm{sgn}(x_2) \\ \omega \end{pmatrix}. \tag{34}$$

The system orbit evolves smoothly in two subspaces defined by the sign of the scalar function $H(x) = x_2$. We can write (34) in the form (4) with

$$F_1 = \begin{pmatrix} x_2 \\ -x_1 + \sin(x_3) - F \\ \omega \end{pmatrix}, \tag{35}$$

$$F_2 = \begin{pmatrix} x_2 \\ -x_1 + \sin(x_3) + F \\ \omega \end{pmatrix}. \tag{36}$$

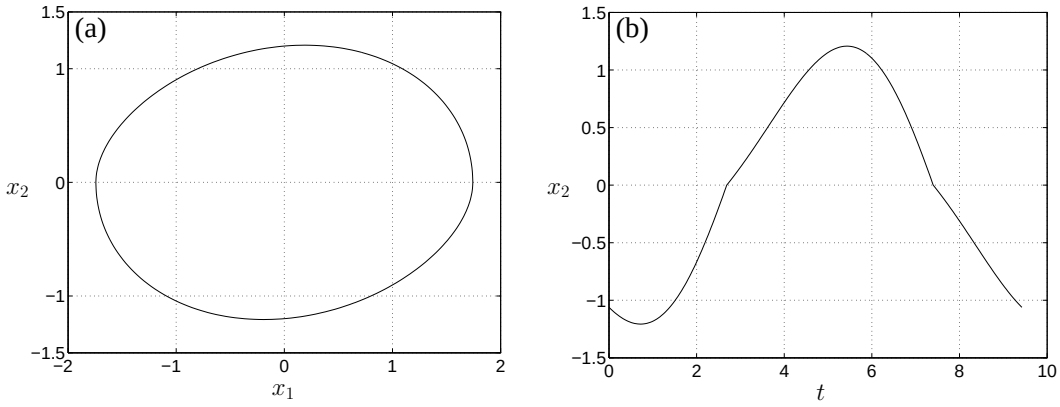

Figure 7: (a) A simple periodic orbit, and (b) corresponding time series of the velocity coordinate for $\omega^{-1} = 1.5$ and $F = 0.3$ (see point '1' in Fig. 8).

In Fig. 7(a) we depict a simple symmetric orbit that is an orbit built from two segments of period $\frac{2\pi}{\omega}$: one segment was generated by the vector field F_1 and the other by the vector field F_2, at parameter values $\omega^{-1} = 1.5$, $F = 0.3$. The time series of the velocity coordinate x_2 is depicted in Fig. 7(b).

Under the variation of the bifurcation parameter F we found that the symmetric orbit undergoes the crossing-sliding bifurcation scenario at $\omega^{-1} = 1.5$ and $F = 0.6656$. Past the bifurcation point two additional sliding segments form part of the orbit.

The aforementioned bifurcation point belongs to a one-parameter crossing-sliding bifurcation curve which we shall term B_α, given by

$$F = \frac{\omega^2}{\omega^2 - 1} \sin\left[\cot^{-1}\left(\frac{\omega \sin(\pi\omega^{-1})}{1 + \cos(\pi\omega^{-1})}\right) + \pi\right] \quad \text{for} \quad \omega \in (0.5,\, \infty),\ \omega \neq 1. \tag{37}$$

If we now follow periodic orbits along B_α it turns out that for $(\omega^{-1},\, F) = (0.5,\, \frac{1}{3})$ the non-degeneracy condition $H_x F_{1x} F_1 > 0$ for the crossing-sliding bifurcation scenario is violated (it becomes zero) and $H_x (F_{1x})^2 F_1 > 0$. Thus the set of analytical conditions determining the degenerate codimension-two crossing-sliding bifurcation is satisfied.

In the case of the degenerate crossing-sliding bifurcations, two curves of codimension-one sliding bifurcations, namely grazing-sliding and switching-sliding (which we shall denote by B_γ and B_β respectively), branch out from the node where B_α terminates. Moreover, B_β and B_γ join B_α in a smooth way; that is $B_\alpha - B_\gamma$ and $B_\alpha - B_\beta$ form at least C^1-differentiable curves in the neighbourhood of the codimension-two node in the two parameter space. This can be seen in Fig. 8 where the three curves B_α, B_β and B_γ are depicted. All the bifurcation curves depicted in the figure were obtained using a numerical continuation technique, based on shooting, developed for sliding bifurcations. Analytical and numerical curves B_α agree with high accuracy and cannot be distinguished in Fig. 8. The crossing of different bifurcation boundaries around the codimension-two node leads to creation of additional segments of the orbit forming a limit cycle but the stability and period of orbits remain unchanged.

Orbits around the node before and after crossing the B_α boundary, for $(\omega^{-1},\, F) = (1.8,\, 0.35)$ and $(\omega^{-1},\, F) = (2,\, 0.35)$ respectively, are depicted in Fig. 9(a) and (b). Subsequent parameter variations such that the orbit crosses B_β will lead to two additional segments of the orbit. Time series of an orbit before, for $(\omega^{-1},\, F) = (2.5,\, 0.2)$, and after, for $(\omega^{-1},\, F) = (2.5,\, 0.15)$, crossing B_β are depicted in Fig. 10. The additional non-sliding segment of the orbit born in the bifurcation is more clearly visible in Fig. 11, which is a zoom into the boxed area depicted in Fig. 10(b).

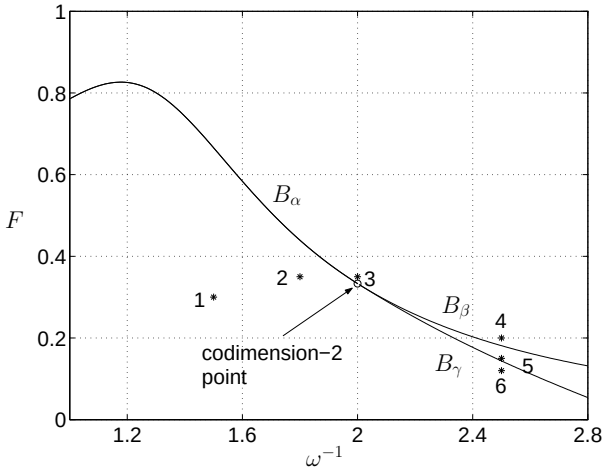

Figure 8: Two parameter bifurcation diagram around the codimension-two node. Asterisks labelled by numbers denote parameter values around the codimension-two point for which the periodic orbits were plotted.

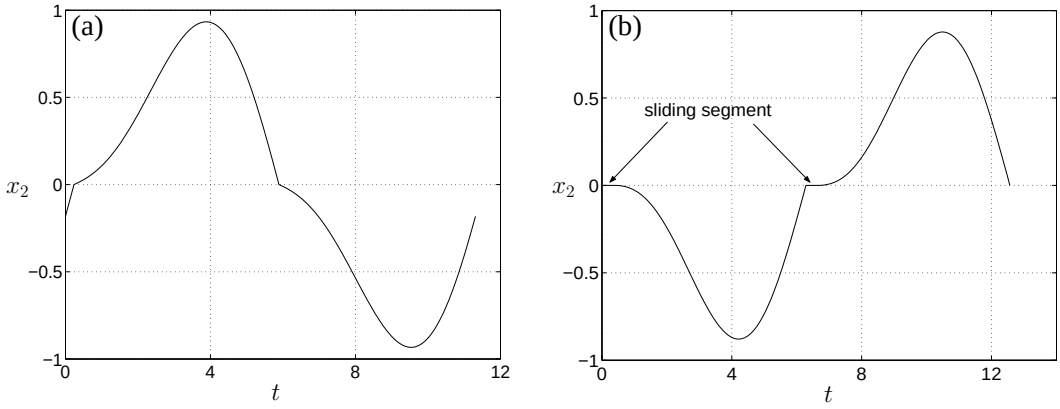

Figure 9: (a) Time series of a simple orbit corresponding to point '2' in Fig. 8, and (b) time series of a limit cycle after crossing-sliding scenario – corresponding to '3' in Fig. 8

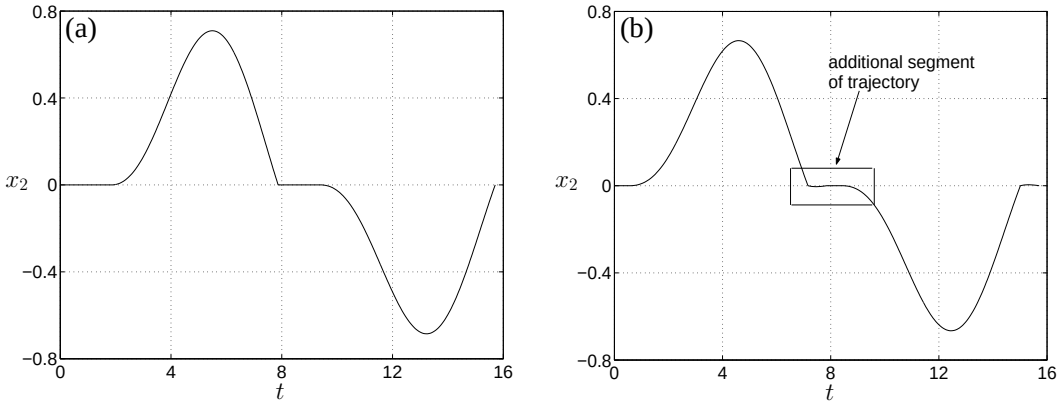

Figure 10: (a) Time series of an orbit corresponding to point '4' in Fig. 8, and (b) time series of a limit cycle after switching-sliding scenario – corresponding to '5' in Fig. 8; boxed area in the figure is magnified in Fig. 11 where additional segment of the orbit born in the bifurcation is visible.

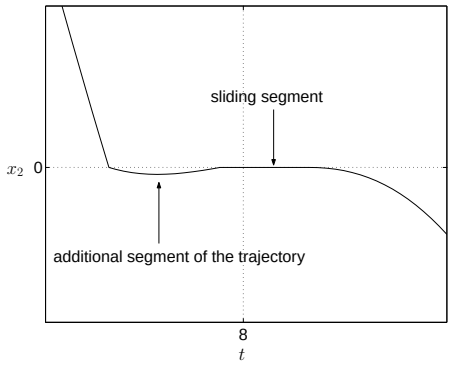

Figure 11: Zoom into the boxed area from Fig. 10(b) depicting additional segment of the orbit born after the switching-sliding bifurcations

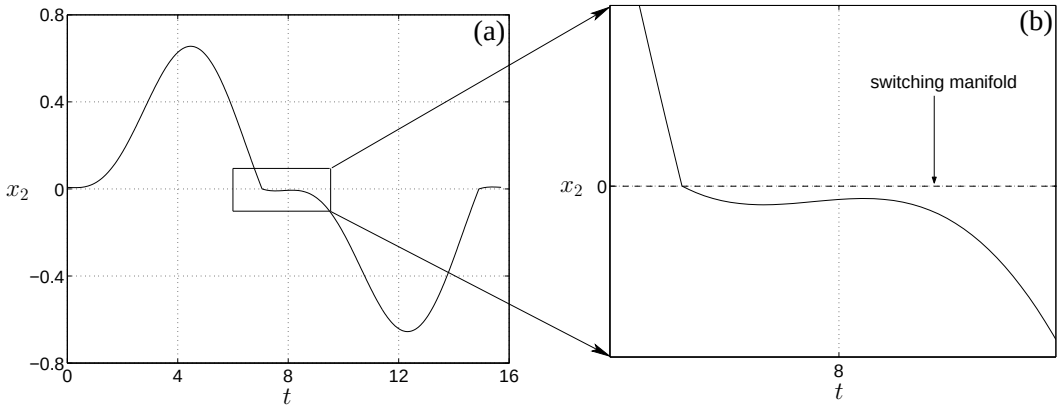

Figure 12: (a) Time series of an orbit corresponding to point '6' in Fig. 8, and (b) zoom into the region where grazing occurs

Finally, we present the time series of the limit cycle under the variation of the bifurcation parameter F such that the boundary B_γ is crossed. After crossing B_γ we enter the region where a simple orbit exists. Such an orbit for the parameters $(\omega^{-1}, F) = (2.5, 0.12)$ is depicted in Fig. 12. Thus, our numerical investigations indeed confirm that the degenerate codimension-two crossing-sliding bifurcation is an origin of three codimension-one sliding bifurcation curves.

4.2 Degenerate corner-collision bifurcations

Let us now focus on external corner-collisions, where one of the non-degeneracy hypotheses (26) that prevent sliding from occurring locally is violated.

4.2.1 Corner-collision with external grazing

We first consider a degenerate case where the vector field F_1 is tangent to Σ_1 at the corner, say $x = \chi$. We can write the defining and non-degeneracy conditions for such a bifurcation as

$$H_{1x}F_1 = 0,$$
$$H_{2x}F_i > 0,$$
$$H_{1x}F_2 < 0.$$

An additional non-degeneracy condition would be required on the curvature of the incoming orbit at the critical point. The simplest case would be that the orbit exhibits a local minimum

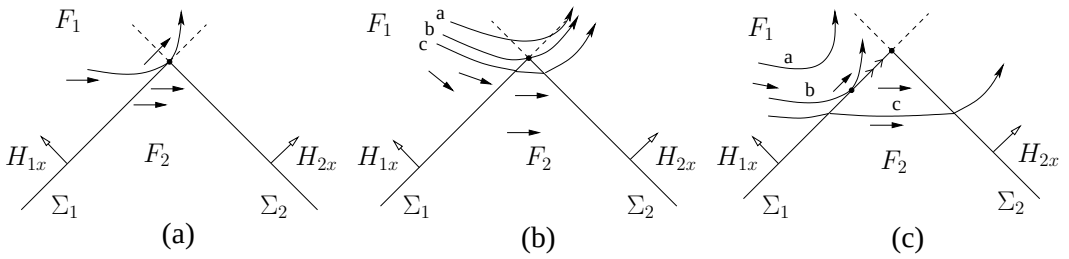

Figure 13: (a) Codimension-two degenerate corner-collision bifurcation and unfolding depicting (b) codimension-one corner-collision and (c) codimension-one grazing-sliding featuring the repelling sliding set.

with respect to Σ_1. This condition can be expressed as

$$\left.\frac{dH_1^2(\Phi_1(x,t))}{dt^2}\right|_{t=0} = H_{1x}F_{1x}F_1 > 0. \tag{38}$$

An unfolding of this codimension-two scenario leads to two codimension-one C-bifurcations: namely a standard codimension-one corner-collision and a grazing-sliding with a repelling sliding set. The later scenario leads to a *catastrophe* — a limit cycle undergoing this type of sliding bifurcation is destroyed by collision with an (infinitely) unstable cycle that evolves along the unstable sliding set. Part of the critical limit cycle featuring degenerate contact with the switching manifold is depicted in Fig. 13(a).

One of the unfoldings, depicting a standard codimension-one corner-collision is illustrated in Fig. 13(b). In the figure, the label 'a' depicts an orbit segment (assumed to be part of a limit cycle) that does not reach the corner. Under parameter variation the limit cycle hits the corner (orbit labelled 'b'). Further parameter variation causes the orbit to hit Σ_1, then switch to being governed by vector field F_2. This scenario is analogous to a standard corner-collision bifurcation.

Another unfolding leads to a grazing-sliding case with a repelling sliding set, where the bifurcating orbit grazes Σ_1 tangentially (orbit 'b' in Fig. 13(c)). Variation of the bifurcation parameter leads the orbit to hit the manifold Σ_1 outside of the sliding subset and then to switch to the vector field F_2. Since F_2 points out from Σ_1, in this case the original limit cycle is destroyed and we encounter a catastrophe.

4.2.2 Corner-collision with internal grazing

Consider instead a case where the a tangency between F_2 and Σ_1 occurs at the degenerate corner-collision. that is $H_{1x}F_2 = 0$ at the codimension-two point. We now have the following defining and non-degeneracy conditions defining this scenario

$$\begin{aligned} H_{1x}F_2 &= 0, \\ H_2F_i &> 0, \\ H_{1x}F_1 &< 0. \end{aligned}$$

In this case we can encounter two distinct codimension-two scenarios depending on the non-degeneracy condition which reflects the curvature of the vector field F_2 with respect to the switching manifold; that is depending on whether F_2 exhibits a local maximum or minimum with respect to Σ_1.

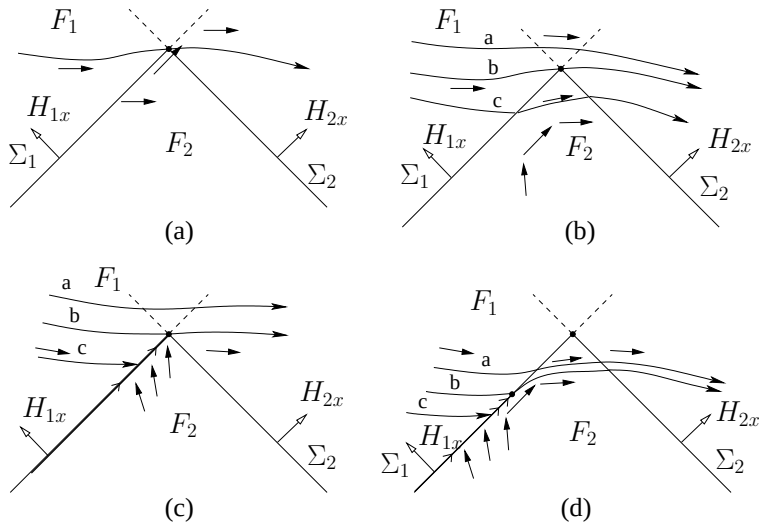

Figure 14: (a) Degenerate codimension-two corner-collision and codimension-one C-bifurcations unfolded from this scenario: (b) standard corner-collision of codimension-one, (c) corner-collision in the presence of sliding, and (d) crossing-sliding bifurcation.

Let us first suppose that F_2 exhibits a local maximum with respect to Σ_1 at the codimension-two point. That is, we require

$$\left.\frac{dH_1^2(\Phi_2(x,t))}{dt^2}\right|_{t=0} = H_{1x}F_{2x}F_2 < 0. \tag{39}$$

Unfolding of this scenario implies that three codimension-one events are possible: a standard corner-collision bifurcation, a crossing-sliding scenario and a corner-collision of codimension-one but with a sliding motion on Σ_1. The third scenario has not been analysed as yet in the literature.

The critical degenerate orbit is sketched in Fig. 14(a) and the unfoldings are schematically depicted in Fig. 14(b), (c) and (d). We use the same standard notation of labelling by 'a' the orbit before, by 'b' at, and by 'c' after the bifurcation.

Fig. 14(b) depicts the standard external corner-collision scenario. Fig. 14(c) depicts in turn a corner-collision scenario, but this time an orbit after the bifurcation instead of following Φ_2 moves along the switching manifold until the corner of the discontinuity set is reached. In Fig. 14(d) we can see an orbit (labelled 'a') crossing Σ_1 transversally. Parameter variation would cause this orbit to hit the boundary of the sliding set formed on Σ_1 and to the creation of an additional sliding segment forming part of an orbit. Thus, we have arrived at a codimension-one crossing-sliding bifurcation (compare with Fig. 2(a)).

Let us now consider the other case, where the flow corresponding to F_2 exhibits a local minimum with respect to Σ_1. The non-degeneracy condition in this case can be expressed as

$$\left.\frac{dH_1^2(\Phi_2(x,t))}{dt^2}\right|_{t=0} = H_{1x}F_{2x}F_2 > 0. \tag{40}$$

Now unfolding of the codimension-two scenario leads to a standard corner-collision and a corner-collision with a switching manifold featuring sliding as depicted for the previous case. There is also a third codimension-one C-bifurcation different from the one observed in the previous case; instead of a crossing-sliding we observe a switching-sliding.

Figure 15(a) depicts the critical orbit at the codimension-two point. The unfolded switching-sliding scenario is depicted in Fig. 15(b). Before the bifurcation the orbit hits Σ_1 within the

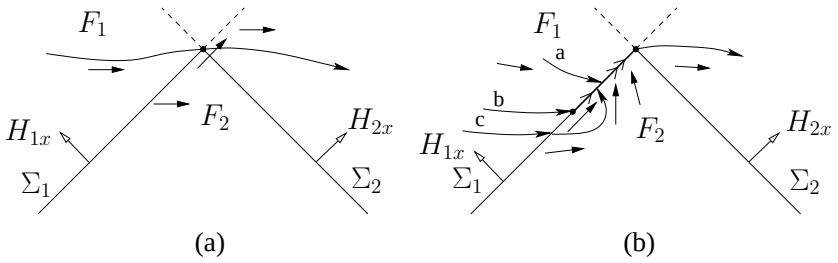

Figure 15: (a) Degenerate codimension-two corner-collision bifurcation and (b) one of the C-bifurcations unfolded from this codimension-two bifurcation.

sliding region (orbit labelled by 'a' in the figure). Variation of the bifurcation parameter leads to an orbit (labelled 'b') which hits the boundary of the sliding region. Further parameter variation leads to formation of an additional orbit segment 'c', generated by F_2, which can be compared with the typical switching-sliding case depicted in Fig. 2(c)).

4.2.3 Example 2: A degenerate corner collision in an artificial model

A full unfolding of the scenarios described above, including the more general case of boundary intersection, rather than a corner-collision, is left for future work. Instead we shall end this section with an example. Note that power electronics has many examples of corner-collision bifurcations which can occur when a component switches on or off, as a result of comparing a signal to a saw tooth. Codimension-one corner-collisions have been found in such systems by a number of authors and shown to undergo many of the dynamical scenarios undergone by border-collision bifurcations of piecewise-linear maps [Yuan et al. 1998, Deane & Hamill 1990, Fossas & Olivar 1996]. In fact, in [di Bernardo et al. 1998] the dynamics of a five-piece chaotic attractor in a DC-DC buck converter was shown to be organised by the near-occurrence of a codimension-two corner collision of a five-periodic orbit. However, in that case the vector fields $F_{1,2}$ are both linear, so that the curvature condition (38) is replaced by equality, leading to a degenerate codimension-two bifurcation where the critical orbit actually slides over an $O(1)$ distance of Σ_1. Small adjustments to this model, to include for example nonlinear corrections to Ohm's law, would lead to the bifurcation scenario described in Sec. 4.2.1 above. Rather than study such a model here, we instead study a canonical model for this bifurcation, which is obtained by explicit construction.

Following [di Bernardo et al. 2001b] we take a system

$$\begin{array}{ll} \left\{ \begin{array}{l} \dot{x} = \gamma \\ \dot{y} = \delta \end{array} \right\} & \text{for } x > 0,\ -x\tan\alpha < y < x\tan\beta \text{ (region } G_1\text{)} \\ \left\{ \begin{array}{l} \dot{r} = \epsilon r(a-r) \\ \dot{\theta} = 1 \end{array} \right\} & \text{otherwise (region } G_2\text{)} \end{array} \tag{41}$$

where

$$x + 1 = r\cos\theta, \quad y = r\sin\theta,$$

and γ, δ, β, ε and a are real constants; see Fig. 16(a).

Consider the system (41). For $a > 0$ there is a limit cycle which is stable if $\varepsilon > 0$. At $a = 1$ this limit cycle collides with the boundary of region G_2 in an external corner collision bifurcation. Specifically we take

$$H_1(x, y) = -y, \quad H_2(x, y) = y\cos\beta - x\sin\beta.$$

Note that the non-degeneracy condition for the corner-collision to be codimension-one is (26) are satisfied provided

$$0 < \alpha, \quad \beta < \pi/2, \quad \delta > \gamma\tan\beta, \quad \delta > -\gamma\tan\alpha. \tag{42}$$

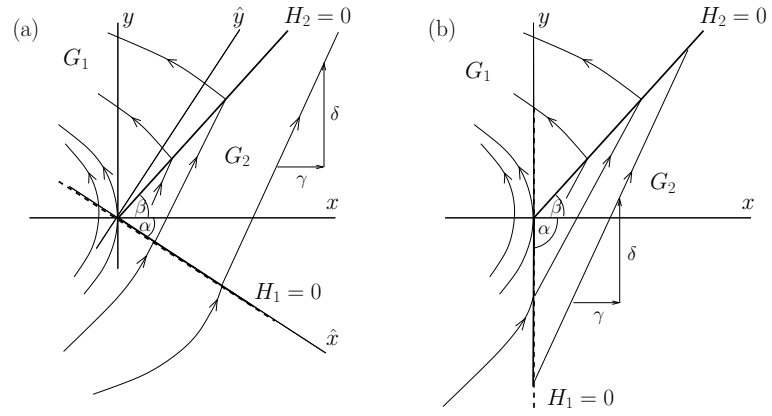

Figure 16: (a) Sketch of the phase portrait of (41) undergoing a codimension-one corner-collision bifurcation at $a = 1$ (b) A codimension-two case defined by $\alpha = \pi/2$.

Since the systems in regions G_1 and G_2 are solvable in closed form one can explicitly construct the Poincaré map $x_0 \mapsto \Pi x_0$ associated with the Poincaré section $\{y = 0, x > -1\}$ (details of the analysis are contained in [di Bernardo et al. 2001b]), and perfect agreement was found with the ZDM. Here we shall just rely on the former approach. After some routine calculation, using the fact that the critical periodic orbit is just $r = 1$, one can linearise and construct the Poincaré map to be:

$$\hat{x} \mapsto N\left(1 - \frac{[\hat{\gamma} + \hat{\delta}\tan\alpha]\tan(\alpha+\beta)}{\hat{\gamma}\tan(\alpha+\beta) - \hat{\delta}}\hat{x}\right) + M\cos\alpha\mu \tag{43}$$

Here $\hat{x}$ is a co-ordinate in the Poincaré section (see Fig. 16)

$$\mu = a - 1, \quad \hat{\gamma} = \gamma\cos\alpha - \delta\sin\alpha, \quad \hat{\delta} = \delta\cos\alpha + \gamma\sin\alpha,$$

and

$$N = \exp(-2\varepsilon\pi), \quad M = (1 - \exp(-2\varepsilon\pi)).$$

Now consider the codimension-two corner bifurcation that occurs when all the conditions (42) are satisfied except $\alpha = \pi/2$. Then the flow F_1, which is locally vertical at the grazing point, becomes precisely tangent to the switching set Σ_1. Thus, in the notation of the above sections, this corresponds to a corner-collision with internal grazing. Looking at the explicitly constructed local Poincaré map (43), we can see immediately that this can no longer be described by the piecewise-linear normal form. This is because the term $\tan\alpha$ becomes infinite, which tells us that the asymptotic expansion used in [di Bernardo et al. 2001b] has become invalid. Instead we should expect to see a map with a jump at higher than the linear order. Maps with such behaviour are known to be able to give rise to the sudden jump to broad-band chaos. Thus a complete unfolding of this degeneracy within the context of this example would seem to be pressing.

Finally it might be pertinent to point out that other codimension-two corner-collisions can be found by breaking other inequalities in (42). For example, by letting $\delta = -\gamma\tan\alpha$, we would get a corner-collision with internal grazing as described in Sec. 4.2.2. However, in order to satisfy one of the non-degeneracy constraints (39) or (40) we would need to adjust the system to make either the vector field F_2 or the manifold Σ_1 nonlinear.

5 Type II: C-bifurcations of degenerate cycles

Here we consider different cases of C-bifurcations of non-hyperbolic orbits. That is eigenvalues (i.e. *Floquet multipliers*) of the Jacobian matrix of a map P built around the periodic point

of the critical orbit, ignoring any contact with Σ, lie on the unit circle. This possibility can easily occur as an additional degeneracy for each of the codimension-one bifurcations described in Sec. 2.1. The complete unfolding of each case remains an open question. However, since the degeneracy is in the global Poincaré map rather than the grazing it should be relatively straightforward to explicitly construct examples in which such codimension-two C-bifurcations occur using a methodology like that of Example 2 above. This is left for future work. Sec 5.1 presents just one case of a non-hyperbolic sliding bifurcation, giving a numerical unfolding for a particular example. Then, in Sec 5.2, we focus on the one case that has been worked out in some detail, that of grazing bifurcations in class **A** systems. We present results by example; more general results will appear elsewhere.

The minimum dimension of phase space where the scenarios described here can be observed is $n = 2$ in the case where an eigenvalue of the map P is 1, and $n = 3$ for eigenvalues -1 or a complex pair at the codimension-two point.

5.1 Example 3: Flip-grazing in a forced nonlinear dry-friction oscillator

Following [Yoshitake & Sueoka 2000, di Bernardo et al. 2003b], consider a dry friction oscillator described by the equation

$$\ddot{x} + x = \alpha_1 \ \mathrm{sgn}(1 - \dot{x}) - \alpha_2(1 - \dot{x}) + \alpha_3(1 - \dot{x})^3 + \alpha_4 \cos(\omega t). \tag{44}$$

Here the positive real constants $\alpha_1, \alpha_2, \alpha_3$ are the coefficients of the kinematic friction characteristics, α_4 is the amplitude of the forcing and ω its angular frequency. Introducing $x_1 = x,\ x_2 = \dot{x},\ x_3 = \omega t (\mathrm{mod} 2\pi)$, we obtain an autonomous Filippov system (4) on the cylinder with

$$F_{1,2}(x) = \begin{pmatrix} x_2 \\ -x_1 \pm \alpha_1 - \alpha_2(1 - x_2) + \alpha_3(1 - x_2)^3 + \alpha_4 \cos(x_3) \\ \omega \end{pmatrix}, \tag{45}$$

and

$$H(x, \alpha) = x_2 - 1. \tag{46}$$

It is known (see [di Bernardo et al. 2003b]) that at

$$\alpha_1 = \alpha_2 = 1.5, \quad \alpha_3 = 0.45, \quad \alpha_4 = 0.1, \quad \omega \approx 1.7078$$

a $\frac{8\pi}{\omega}$-cycle exists in the region $H(x, \alpha) < 0$, and touches the discontinuity boundary Σ (see Fig. 17). This is a grazing-sliding bifurcation of the system. Starting with the numerical solution corresponding to Fig. 17, one can continue this bifurcation in two control parameters α_4 and ω.

It turns out that a branch denoted by TCH_2 in the (α_4, ω) plane, presented in Fig. 18, corresponding to a family of $\frac{8\pi}{\omega}$-cycles undergoing the grazing-sliding bifurcation terminates at some point $A_1 = (\alpha_4, \omega) \approx (1.324, 2.548)$. At this point a limit cycle with period $\frac{8\pi}{\omega}$ undergoes a period-doubling bifurcation. To be precise we observe a period doubling of a $\frac{4\pi}{\omega}$-cycle which at A_1 becomes an $\frac{8\pi}{\omega}$-cycle for decreasing values of the bifurcation parameter α_4. Thus, at A_1 the periodically forced dry-friction oscillator exhibits a codimension-two bifurcation when a nonhyperbolic $\frac{4\pi}{\omega}$-cycle touches the discontinuity set.

A bifurcation curve corresponding to a family of limit cycles characterised by $\frac{4\pi}{\omega}$-period was then followed in the (α_4, ω) parameter space. This bifurcation curve is denoted as TCH_1 in Fig. 18. Another branch point was detected at $A_2 = (\alpha_4, \omega) \approx (2.814,\ 3.034)$, where the grazing cycle undergoes a period-doubling bifurcation. Finally, Fig. 18 contains a curve PD_1 emanating from point A_1 on which the smooth flip (period-doubling) bifurcation of the $\frac{4\pi}{\omega}$-cycle occurs.

Limit cycles depicting qualitatively different types of orbits around the codimension-two point are presented in Fig. 19. A $\frac{4\pi}{\omega}$-cycle depicted in Fig. 19(a) was obtained for the parameter

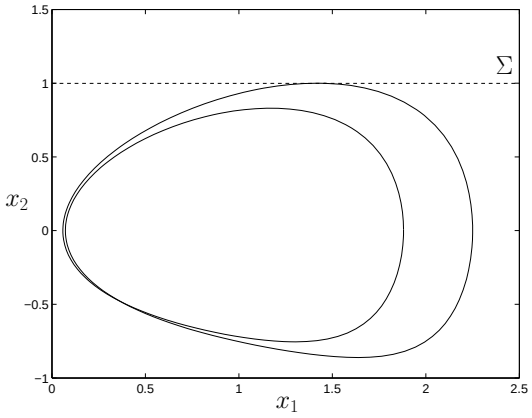

Figure 17: A grazing cycle of the periodically forced dry-friction oscillator (44).

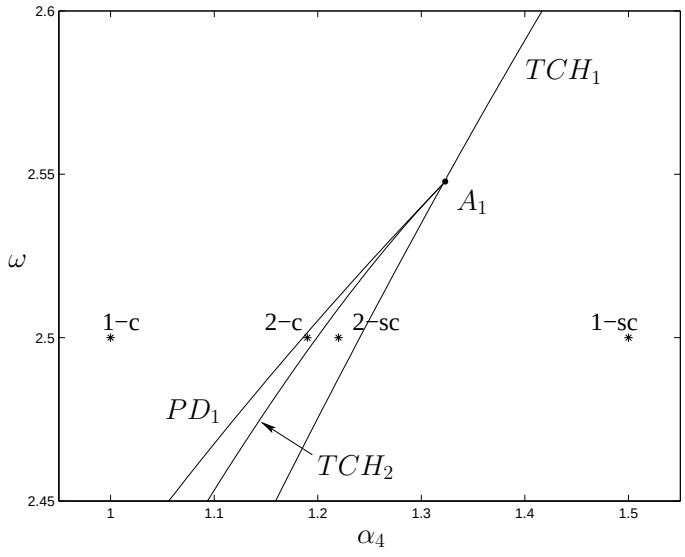

Figure 18: Bifurcation curves of (44): TCH_1 - grazing-sliding bifurcation of the $\frac{4\pi}{\omega}$-cycle; PD_1 - flip (period-doubling) bifurcation of the $\frac{4\pi}{\omega}$-cycle; TCH_2 - grazing-sliding bifurcation of the $\frac{8\pi}{\omega}$-cycle; $A_{1,2}$ - codimension-two flip-grazing points.

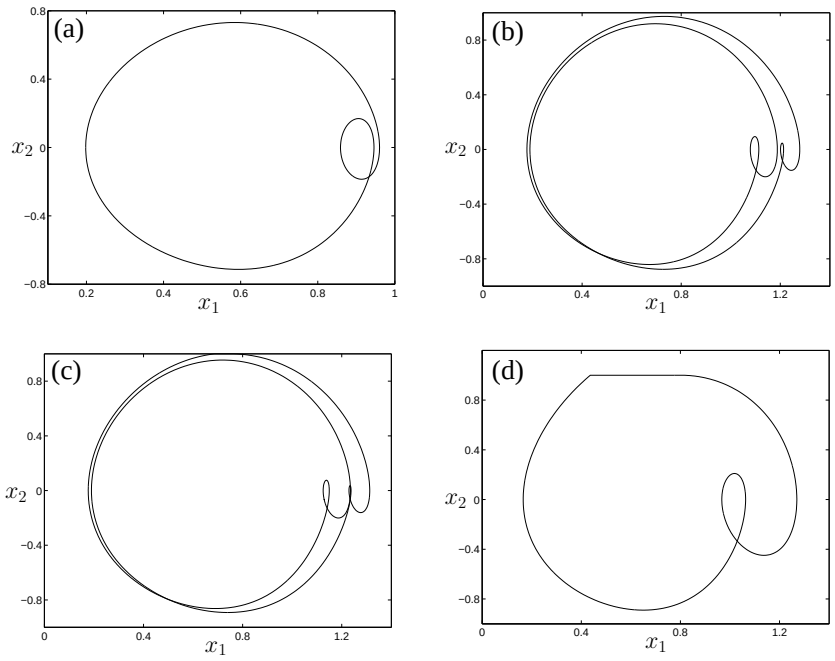

Figure 19: Qualitatively different types of limit cycles around the codimension-two bifurcation point detected for $\alpha_1 = \alpha_2 = 1.5$, $\alpha_3 = 0.45$, $\omega = 2.5$, and (a) $\alpha_4 = 1$, (b) $\alpha_4 = 1.19$, (c) $\alpha_4 = 1.22$ and (d) $\alpha_4 = 1.5$.

values corresponding to point '1-c' in Fig. 18. Under the variation of α_4 this limit cycle will cross the branch PD_1. Thus, it will undergo period doubling. An orbit with double period at point '2-c' in Fig. 18 is depicted in Fig. 19(b). Further variation of α_4 leads the to the period-two orbit undergoing a grazing-sliding bifurcation (crossing of TCH_2). In our current example the $\frac{8\pi}{\omega}$-cycle after grazing-sliding scenario preserves its stability and period, and acquires a 'sliding' segment. Such an $\frac{8\pi}{\omega}$-cycle with a sliding segment is depicted in Fig. 19(c) (at point '2-sc' in Fig. 18). Finally, further increase of α_4 leads to another grazing-sliding scenario when the curve TCH_1 is crossed. In this bifurcation the period-two orbit with sliding disappears and a $\frac{4\pi}{\omega}$-cycle with sliding is born. Such limit cycle with a sliding segment is depicted in Fig. 19(d) (point '1-sc' in Fig. 18). It is worth noting that the grazing-sliding scenario occurring along TCH_1 on either side of A_1 leads to two distinct bifurcation scenarios. If TCH_1 is crossed on the right from A_1 (for $\alpha_4 > 1.324$ we observe a continuous transition from a $\frac{4\pi}{\omega}$-cycle with sliding to a $\frac{4\pi}{\omega}$-cycle without sliding or vice versa, depending whether parameter ω is increased or decreased). On the other hand if TCH_1 is crossed on the left from A_1 (for $\alpha_4 < 1.324$) we observe a transition from a stable $\frac{4\pi}{\omega}$-cycle with sliding to an unstable $\frac{4\pi}{\omega}$-cycle without sliding. This scenario is accompanied by a birth of a stable $\frac{8\pi}{\omega}$-cycle with sliding (if ω is decreased we observe a transition to a limit cycle with sliding and disappearance of a period-two orbit).

5.2 Example 4: Non-hyperbolic grazings in a forced impact oscillator

Consider now an example of a class **A** system which models a periodically forced mechanical single-degree of freedom oscillator that can impact with a rigid stop. It has three state variables, where x_1 is position, x_2 velocity and $x_3(\mathrm{mod}2\pi)$ is the driving phase.

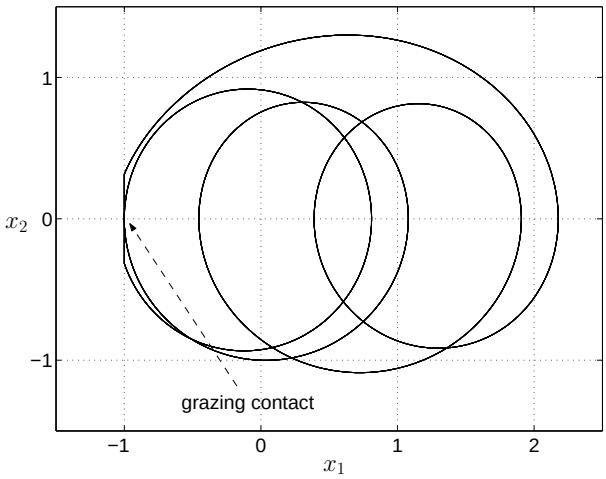

Figure 20: Grazing orbit with $\lambda = 1$

The system is assumed to obey the ODE system

$$\dot{x}_1 = x_2 \tag{47}$$

$$\dot{x}_2 = -\frac{1}{w^2}x_1 - \frac{2d}{w}x_2 + A\left(\left[\frac{1}{w^2} - 1\right]\cos(x_3) - \frac{2d}{w}\sin(x_3)\right) \tag{48}$$

$$\dot{x}_3 = 1 \tag{49}$$

for $x_1 > -1$, with the rigid stop being at $x_1 = -1$. At the stop, a Newton restitution law is assumed

$$x_2^+ = -rx_2^- \,, \tag{50}$$

where x_2^- is the incoming velocity, immediately prior to impact, and x_2^+ is the outgoing velocity instantaneously later. The dimensionless parameters of the system are: d which represents the damping coefficient, w the ratio of the driving frequency to the undamped natural frequency, r the coefficient of restitution, and A the amplitude of the trivial periodic response of the system (the particular integral solution). When $0 < A < 1$ the system admits the non-impacting periodic solution

$$x_1 = A\cos(x_3), \qquad x_2 = -A\sin(x_3),$$

which is stable if $d > 0$ and $w > 0$. Besides this solution, the system may have additional impacting periodic solutions and chaotic attractors as described in many previous works, e.g. [Peterka 1974a, Nordmark 2002, Budd & Dux 1994].

5.2.1 Non-hyperbolic grazing solution with multiplier $\lambda = 1$

For the parameter values $d = 0.6,\ w = 4.519798,\ A = 0.938042,\ r = 1$ there exists a periodic orbit with one non-grazing impact and one grazing as shown in Figure 20. If the system is linearised around a periodic point of the limit cycle, ignoring the grazing impact, it is characterised by one multiplier $\lambda = 1$. The second non-trivial multiplier is positive and close to zero. The period of the orbit is 8π.

One point on the orbit is $(x_1, x_2, x_3) = (-1, 0.315637, 2.787732)$. In a parameter diagram where w and A are varied, (Figure 21) we find that several one-parameter curves meet at the two-parameter point. There is a curve 'a'–'b' of grazing periodic orbits, and a curve 'c' of saddle-node bifurcations. For this system, there is a stable periodic orbit similar to the two-parameter orbit in the region between curves 'b' and 'c', and at 'b' it undergoes a grazing bifurcation leading to a chaotic attractor similar to the two-parameter orbit (Fig. 20) in a small region above curve

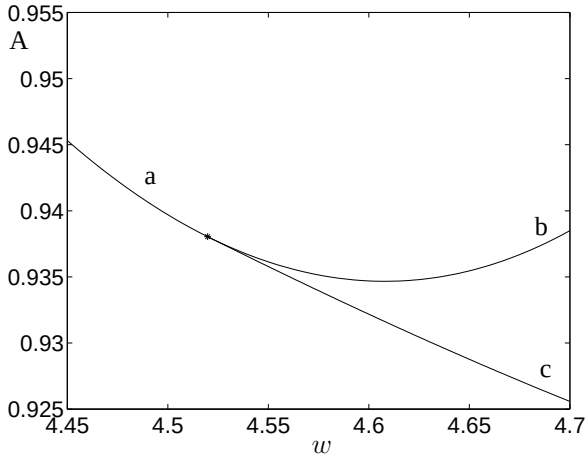

Figure 21: Parameter diagram around the codimension-two point(asterisk). A curve of grazing periodic orbits with a multiplier $\lambda > 1$ is denoted by 'a', and with a multiplier $\lambda < 1$ by 'b'. A curve of non-hyperbolic orbits with a multiplier $\lambda = 1$ characterised by no low velocity impacts is denoted by 'c'.

'b'. Further increases of the parameter A make the attractor disappear in a boundary crisis. The curve where this happens is not included in the diagram. Below 'c' and below and above 'a' there is no attractor close to the two-parameter orbit.

5.2.2 Non-hyperbolic grazing solution with multiplier $\lambda = -1$

For the parameter values $d = -0.3$, $w = 3.729986$, $A = 0.257040$, $r = 0.15$ there exists a periodic orbit with one non-grazing impact and one grazing, as shown in Figure 22. If the system is linearised around the periodic point of the limit cycle, ignoring the grazing impact, it is characterised by one multiplier $\lambda = -1$. The other non-trivial multiplier is negative and its value is around -0.47. One point on the orbit is $(x_1, x_2, x_3) = (-1, 0.170869, 5.186351)$, and the period of the orbit is 6π.

In a parameter diagram where w and A are varied, (Figure 23) we find that several one-parameter curves meet at the two-parameter point. There is a curve 'a'–'b' of grazing period 6π orbits, a curve 'c' of supercritical period-doubling bifurcations, and a curve 'd' of grazing period 12π orbits. For this system, there is a stable periodic orbit similar to the two-parameter orbit (Fig. 22) in the region below curves 'a' and 'c'. At 'c' there is a supercritical period-doubling bifurcation, branching off a stable orbit of twice the period. At 'd' this orbit becomes grazing. The stability characteristics of this orbit changes quite rapidly along the curve 'd'. Near the two-parameter point one multiplier must be close to one, but at the right edge of the diagram, the multipliers are already complex. Similar changes take place on curve 'a'. In this system, the grazing bifurcation at 'd' does not continuously create an attractor.

6 Type III: Simultaneous occurrence of two grazings

In this section we consider codimension-two C-bifurcations characterised by two nonsmooth transitions occurring simultaneously at two different points in the phase space along the orbit. Any pair of sliding bifurcations, grazing-bifurcations or corner-collisions occurring at two spatially separated points along the orbit leads to this class of codimension-two C-bifurcation.

We also include in this type any pair of sliding, grazing, corner-collisions where the system under consideration features two switching surfaces and the two spatially separated bifurcation

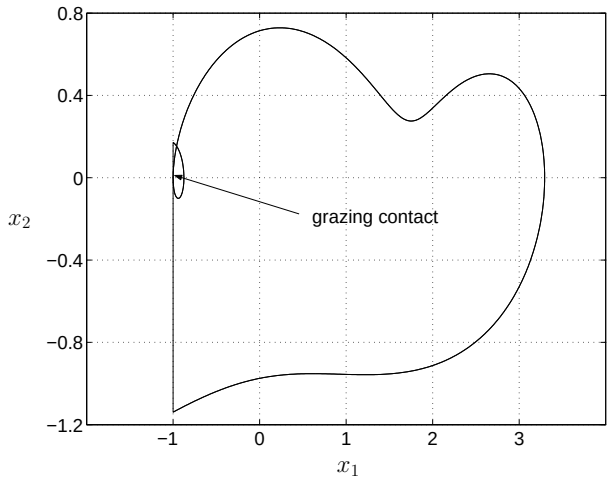

Figure 22: Grazing orbit with $\lambda = -1$

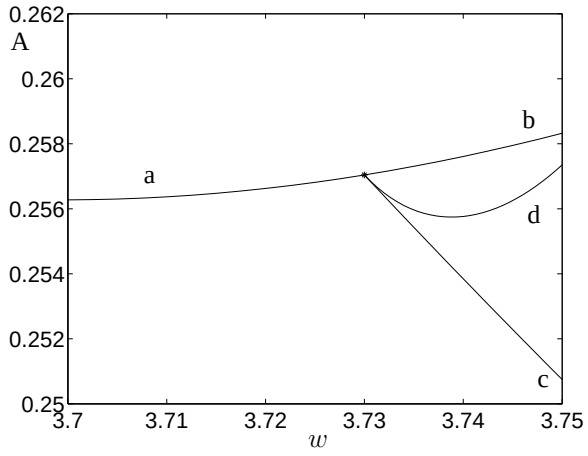

Figure 23: Parameter diagram around the codimension-two point (asterisk). Curve of grazing periodic orbits with a multiplier $\lambda > -1$ or complex is denoted by 'a', and with a multiplier $\lambda < -1$ by 'b'. Curve denoted by 'c'corresponds to a branch of limit cycles with $\lambda = -1$ and no low velocity impacts. Curve 'd' denotes grazing cycles of the double period.

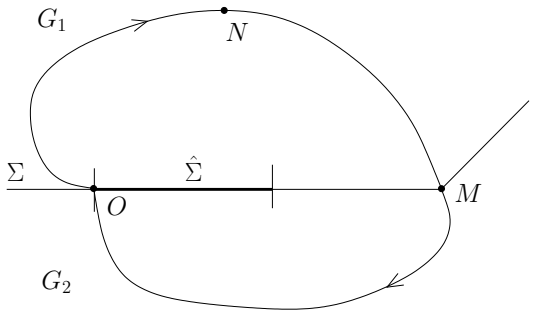

Figure 24: Schematic representation of an orbit undergoing corner-collision (point M) and crossing-sliding (point O) bifurcations

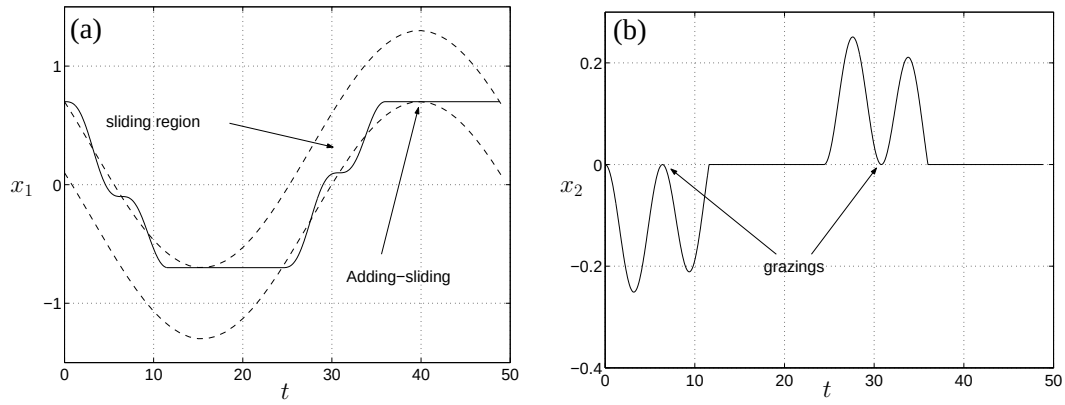

Figure 25: Time series of (a) the position component of the system (33) (b) the velocity component for $\omega^{-1} = 7.76990,\ F = 0.299984$.

scenarios occur on these distinct surfaces. Note that we do not place any constraints on whether surfaces cross transversally or do not cross at all.

As an example consider a limit cycle undergoing a simultaneous occurrence of corner-collision and crossing-sliding bifurcations. Such an orbit is schematically depicted in Fig. 24. This orbit can be studied by appropriate composition of mappings built around any periodic point of the orbit, for instance around point N. The ZDM normal form for codimension-one C-bifurcations can then be used to appropriately obtain a Poincaré map capturing the dynamics of the bifurcating cycle.

We shall now give an example of a system where a codimension-two C-bifurcation of the type considered in the current section was observed.

6.1 Example 5: Combined adding- and grazing-sliding in the linear dry-friction oscillator

We consider the dry-friction oscillator (33), focusing this time on a codimension-two situation where adding-sliding and grazing-sliding occur at two distinct points along a limit cycle. Such a codimension-two bifurcation point has been located at $\omega^{-1} = 7.76990,\ F = 0.299984$, with the grazing-sliding occurring at $x = 0.100044137,\ \dot{x} = 0.\ \omega t = 0.411547546$ and the adding-sliding at $x = 0.700016,\ \dot{x} = 0, \omega t = \frac{\pi}{2}$. The period of the bifurcating orbit is equal to $T = \frac{2\pi}{\omega} = 15.53980\pi$.

Time series of an orbit exhibiting the aforementioned adding-sliding and grazing-sliding bifurcation scenarios are depicted in Fig. 25. Projection onto the switching manifold Σ depicting

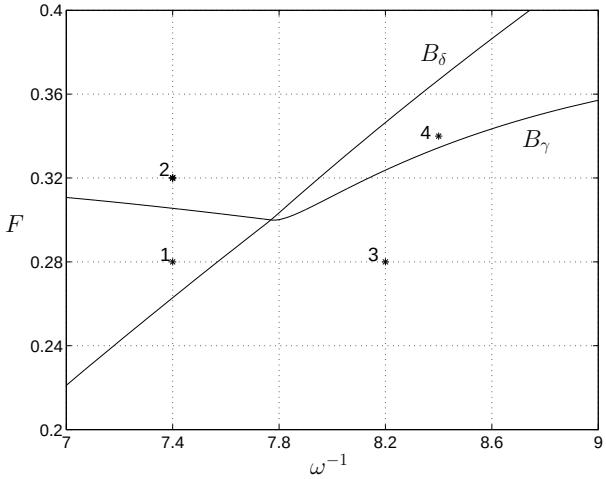

Figure 26: Two-parameter bifurcation diagram around the codimension-two node. B_γ denotes a branch of grazing-sliding and B_δ a branch of adding-sliding bifurcations that cross at the codimension-two point.

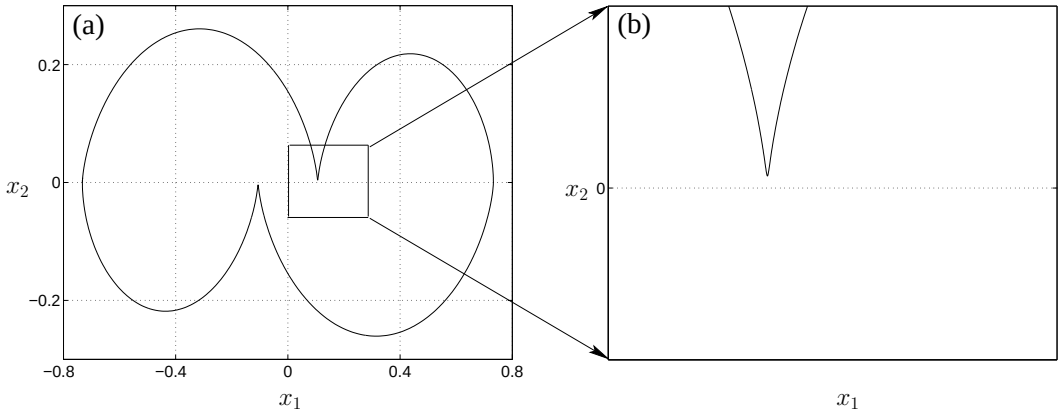

Figure 27: (a) A limit cycle close to the codimension-two point obtained for $\omega^{-1} = 7.4$ and $F = 0.28$ (see asterisk '1' in Fig 26), and (b) zoom into the region where grazing contact occurs

the position component (Fig. 25(a)) allows us to highlight an instant of the adding-sliding taking place at some point along the orbit. A graph of the velocity component (Fig. 25(b)) captures the grazing-sliding interaction. Parameter variations of the bifurcation parameters F and ω will cause the orbit to cross the grazing-sliding and the adding-sliding boundaries in the two-parameter space. Depending on the character of the ZDM map which captures the dynamics of the system a limit cycle undergoing a grazing-sliding scenario might be destroyed. Therefore, generically at a codimension-two point under consideration a branch of adding-sliding bifurcations might terminate at the codimension-two point. However, in our dry-friction oscillator example such a situation does not occur and a stable orbit exists in all regions around the codimension-two point. A bifurcation diagram depicting branches of grazing and adding-sliding which cross at the codimension-two point are presented in Fig. 26. A limit cycle near the codimension-two point is depicted in Fig. 27(a). Note part of the orbit close to the grazing contact (Fig. 27(b)). Variation of any of the two bifurcation parameters might lead the orbit to cross the bifurcation boundaries B_δ or B_γ (which denote the adding-sliding and grazing-sliding boundaries respectively) and hence acquire additional segments which form a limit cycle. A limit cycle after crossing B_γ for increasing values of F leads to an orbit depicted in Fig. 28(a),

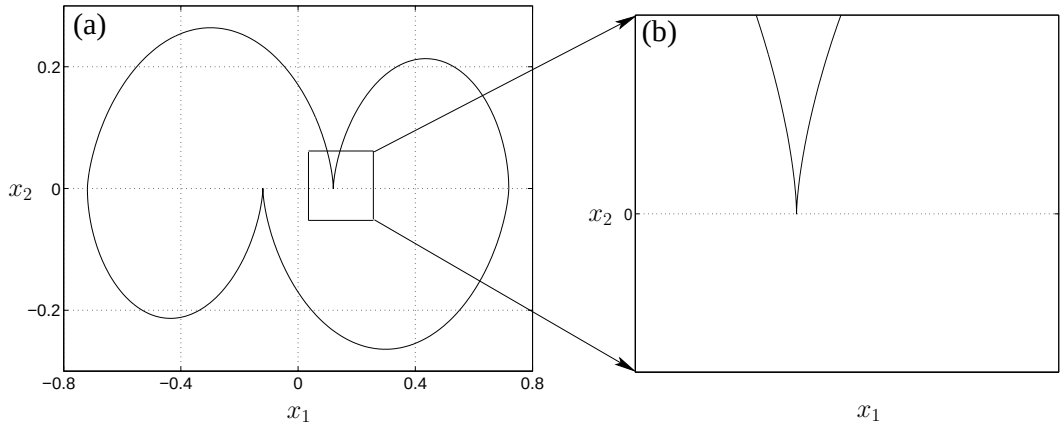

Figure 28: (a) A limit cycle close to the codimension-two point obtained for $\omega^{-1} = 7.4$ and $F = 0.32$ (see asterisk '2' in Fig. 26), and (b) zoom into the region where grazing contact occurs.

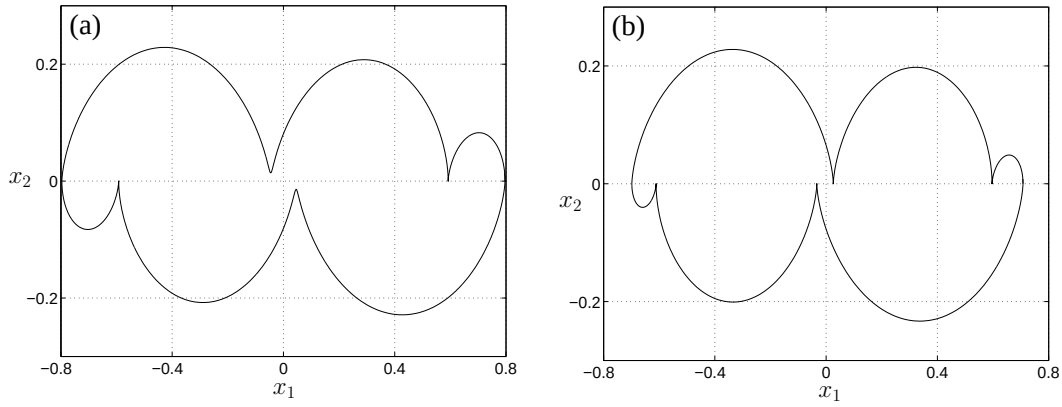

Figure 29: (a) A limit cycle for $\omega^{-1} = 8.2$ and $F = 0.34$ corresponding to asterisk '3' in Fig. 26 and (b) a limit cycle for $\omega^{-1} = 8.4$ and $F = 0.34$ corresponding to asterisk '4' in Fig. 26

with a zoom into the region where the grazing contact occurs shown in Fig. 28(b). To complete our description in Fig. 29 we show two orbits to the right of the curve B_δ that is after the adding-sliding bifurcations take place. Additional "non-sliding" segments, which form small "lobes" in the phase plots of the limit cycles, are clearly visible.

7 Conclusion

In the paper we have presented a first attempt to introduce a framework for a classification of local grazing bifurcations of limit cycles of codimension-two. We have established three broad types of such nonsmooth transitions, where in each case we think of a codimension-one scenario and make it degenerate. This can be done by either: (Type I) making the one of the vector fields at the grazing point be degenerate, (Type II) making the reinjection map along the limit cycle be degenerate, or (Type III) allowing two independent grazing events happen to the same limit cycle. For each type of bifurcation, we have attempted to motivate what this might mean in an application by investigating at least one case in more detail, by providing a commentary on what one should expect to see, backed up by analytical results together with numerical simulations and bifurcation diagrams.

Nonsmooth systems in one of the three classes outlined in Sec. 1, are becoming more and

more important in applications, see for example the reviews [di Bernardo et al. 2004, Brogliato 1999, Zhusubaliyev & Mosekilde 2003]. As with smooth bifurcations, one of the reasons for studying codimension-two C-bifurcations is that they act as organising centres for bifurcations in PWS systems. Obviously, knowledge of the structure of bifurcation curves in parameter space is of practical importance for scientists and engineers who investigate the dynamic behaviour of systems. Therefore we hope that the current work will serve as an initial step towards more in-depth parameter studies of nonsmooth systems arising in applications.

Again, judging from experience with smooth bifurcations, another vital ingredient necessary to carry apply the above theory to applications is a robust numerical framework for analysing both regular and C-bifurcations in piecewise smooth systems. Software such as AUTO [Doedel, et al. 1997] and CONTENT [Kuznetsov & Levitin 1995-1997], when used in standard mode will in general fail at grazing points. Instead one needs to build up a suite of routines that are specifically designed to compute through discontinuity sets, to accurately detect points of intersections with them, and to detect and follow parameter values at which grazings occur. Several such approaches are currently being developed, and have been used to produce the numerical pictures in this paper [Piiroinen & Kuznetsov 2005]. In specific applications where the systems concerned are piecewise linear, one can compute system orbits explicitly and the computation of periodic orbits is reduced to the solution of transcendental equations for the unknown times at which discontinuity sets are hit. For example, in [di Bernardo et al. 2001b] just such an approach was used to compute orbits of example 2, in Sec.4.2.3. The general technique, however, has a much longer history [Peterka 1974a, Feigin 1970] and includes recent studies in power electronics [Zhusubaliyev & Mosekilde 2003], where in depth two-parameter diagrams have been computed. A more general idea is to partition the computation of a limit cycle that crosses say N smooth regions G_i and slides along M discontinuity boundaries Σ_{ij} into $N + M$ separate smooth problems with matching boundary conditions. Then one can use any smooth two-point boundary-value solver to compute the resulting boundary-value problem. This is the philosophy behind SLIDECONT [Dercole & Kuznetsov 2002 [to appear in *ACM TOMS*]] that was used to perform the computations in example 3 (Sec. 5.1). This approach leads to accurate computation of orbits, but can be hard to implement in practice, particularly when many switches occur. Another method is to use shooting-type methods which solve boundary-value problems via Newton's method applied to the Poincaré map. At each discontinuity set encountered by an orbit, discontinuity mappings can be constructed in order to find the tangent direction for nearby orbits. For the first steps in this direction see [Adolfsson, et al. 2001, Dankowicz & Piiroinen 2002] and also the software produced by SICONOS [http://www.enm.bris.ac.uk/staff/ptp/SICONOS_WP4/ 2005, Piiroinen 2005], which also implements complementarity solvers (see e.g. [Brogliato, et al. 2002]) that can deal with discontinuous systems directly. Many problems in the numerical analysis of nonsmooth systems remain to be solved.

A few words might be pertinent on the dynamics that are implied by the presence of the codimension-two points that we have studied. We have, quite deliberately, kept away from a focus on chaotic dynamics in this paper. Clearly there will be chaotic dynamics in a neighbourhood of many of the bifurcations we have described. Perhaps the nature of the chaos known to be created in codimension-one grazing bifurcations (e.g. [Kowalczyk 2005, Banerjee, et al. 1998]) will be greatly transformed by the presence of the codimension-two point. We already mentioned, in Sec. 4.2 the case of a DC-DC converter where the very nature of the observed chaotic dynamics over a wide range of parameter values is organised by a nearby codimension-two corner-collision bifurcation [di Bernardo et al. 2001b]. Other codimension-two bifurcations might cause a *side-switching* in the direction of bifurcation of the simplest periodic orbit; see for example the recent work of Zhao and Dankowicz [Dankowicz & Zhao 2004, Zhao & Dankowicz 2004] who find just such an event in a class **A** system. Other codimension-two bifurcations may cause the transition from a regular bifurcation to a catastrophe, where there is no local attractor. Such would be the case in any region of parameter space where the limit cycle is forced to pass through a region

of repelling sliding motion. At the other extreme, some codimension-two C-bifurcations have almost no influence on the observed dynamics. For instance, in example 1 (Sec. 4.1.3) there is a single periodic attractor in the entire neighbourhood of the codimension-two point. The various codimension-one bifurcation curves that emerge from the codimension-two point just cause the limit cycle to change its topology with respect to the discontinuity set, but such topological changes do not necessarily imply topological changes in phase portrait view in the large.

It must be stressed that our current work is not aimed at giving a complete theory for codimension-two C-bifurcations of limit cycles. It should rather serve as a guideline for the development of such a consistent theory. Clearly, taking even just the restricted class of scenarios we have covered, there remains much to be done, and open problems have been highlighted in the course of the preceding discussion It is worthwhile to note, though, that there are many other possible kinds of codimension-two C-bifurcations. For example, there is a growing literature on piecewise smooth systems that have equilibria precisely on the boundary between two smooth regions and for which nonsmooth analogues of Hopf bifurcations can be proved [Giannakopoulos & Pliete 2001, Kuznetsov et al. 2002]. To embed such systems smoothly into class **A** or **B** above, one would need to add a second parameter to move the equilibrium off the boundary, thus creating a codimension-two event. There are also examples of codimension-one bifurcations of invariant tori, e.g.[Dankowicz, et al. 2002]. In particular, in the work of Zhushubalyev and Mosekilde [Zhusubaliyev & Mosekilde 2003], an intricate two-parameter bifurcation diagram is drawn in a neighbourhood of Neimark-Sacker bifurcations that creates a torus, in a particular system derived from power electronics. Here there are numerous codimension-two points when resonance points on the torus interact with the discontinuity boundary. Neither have we considered any global bifurcations. Clearly grazing limit cycles can become homoclinic, or homoclinic orbits can become degenerate by grazing, or by the equilibrium approaching a discontinuity set, or boundary equilibria can have stable and unstable manifolds which connect to them in *finite time* [Kuznetsov et al. 2002]. Stable and unstable manifolds of limit cycles can also form sudden transverse intersection through interaction with a boundary. The possibilities seem almost endless. If nothing else, we hope this paper serves to stimulate more work into a fascinating, wide open, area of dynamical systems research that is clearly vital from the point of view of applications.

Acknowledgements

The current paper is an outcome of the meeting on codimension-two bifurcations in nonsmooth dynamical systems, which was held at the University of Bristol on the 25th and 26th of July 2003.

The authors gratefully acknowledge support from the EPSRC (Bristol Centre for Applied Nonlinear Mathematics – grant no. GR/R72020) and the European Union (FP5 Project SICONOS IST-2001-37172).

References

J. Adolfsson, et al. (2001). '3D passive walkers: Finding periodic gaits in the presence of discontinuities'. *Nonlinear Dynamics* **24**:205–229.

J. P. Aubin & A. Cellina (1984). *Differential Inclusions*. Springer–Verlag, New York.

S. Banerjee & G. C. Verghese (2001). *Nonlinear phenomena in power electronics*. IEEE Press.

S. Banerjee, et al. (1998). 'Robust Chaos'. *Physical Review Letters* **80**(14).

N. Bautin & E. Leontovich (1976). *Methods and Techniques for Qualitative Analysis of Dynamical Systems on the Plane*. Nauka, Moscow. [in Russian].

B. Brogliato (1999). *Nonsmooth Mechanics – Models, Dynamics and Control*. Springer–Verlag, New York.

B. Brogliato, et al. (2002). 'Numerical simulation of finite dimensional multibody nonsmooth mechanical systems'. *ASME Applied Mechanics Reviews* .

C. Budd & F. Dux (1994). 'Intermittency in impact oscillators close to resonance'. *Nonlinearity* **7**:1191–1224.

W. Chin, et al. (1994). 'Grazing bifurcations in impact oscillators'. *Physical Review E* **50**:4427–4444.

H. Dankowicz & A. B. Nordmark (1999). 'On the origin and bifurcations of stick-slip oscillations'. *Physica D* **136**:280–302.

H. Dankowicz, et al. (2002). 'Low-velocity impacts of quasiperiodic oscillations'. *Chaos Solitons and Fractals* (14):241–255.

H. Dankowicz & P. T. Piiroinen (2002). 'Exploiting discontinuities for stabilization of recurrent motions'. *Dynamical Systems* **17**:317–342.

H. Dankowicz & X. Zhao (2004). 'Local analysis of codimension-one and codimension-two grazing bifurcations in impact microactuators'. submitted to Physica D.

J. H. B. Deane & D. C. Hamill (1990). 'Analysis, simulation and experimental study of chaos in the buck converter'. In *Proceedings of the Power Electronics Specialists Conf. (PESC 1990)*, pp. 491–8, New York, IEEE Press.

F. Dercole, et al. (2003). 'Numerical sliding bifurcation analysis: An application to a relay control system'. *IEEE Trans. Circuits Systems I Fund. Theory Appl.* **50**:1058–1063.

F. Dercole & Yu.A. Kuznetsov (2002 [to appear in *ACM TOMS*]). 'SlideCont: An Auto97 driver for sliding bifurcation analysis'. Preprint nr. 1261, Department of Mathematics, Utrecht University, The Netherlands.

M. di Bernardo, et al. (2005). 'Bifurcations and chaos in piecewise smooth systems; theory and application'. Book to be published by Springer-Verlag.

M. di Bernardo, et al. (2004). 'A review of codimension-one nonsmooth bifurcations'. Submitted to *SIAM Review*.

M. di Bernardo, et al. (2001a). 'Normal form maps for grazing bifurcations in n-dimensional piecewise-smooth dynamical systems'. *Physica D* **160**:222–254.

M. di Bernardo, et al. (2001b). 'Corner-Collision implies Border-Collision Bifurcation'. *Physica D* **154**:171–194.

M. di Bernardo, et al. (1998). 'Grazing, skipping and sliding: analysis of the nonsmooth dynamics of the DC/DC buck converter'. *Nonlinearity* **11**:858–890.

M. di Bernardo, et al. (1999). 'Local Analysis of C-bifurcations in n-dimensional piecewise smooth dynamical systems'. *Chaos, Solitons and Fractals* **10**:1881–1908.

M. di Bernardo, et al. (2003a). 'Bifurcations in Piecewise-Smooth Feedback Systems'. Accepted for publication in International Journal of Control.

M. di Bernardo, et al. (2003b). 'Sliding bifurcations: a novel mechanism for the sudden onset of chaos in dry-friction oscillators'. *International Journal of Bifurcation and Chaos* **13**(10):2935–2948.

M. di Bernardo, et al. (2002). 'Bifurcations of Dynamical Systems with Sliding: derivation of normal form mappings'. *Physica D* **170**:175–205.

E. Doedel, et al. (1997). 'AUTO97: Continuation and Bifurcation Software for Ordinary Differential Equations (with HomCont), User's Guide'. Concordia University, Montreal, Canada.

J. S. Fedosenko & M. I. Feigin (1972). 'On the theory of the slipping state in dynamical systems with collisions'. *Journal of Applied Mathematics and Mechanics (Prikladnaya Matematika i Mechanika)* **36**(5):840–850.

M. I. Feigin (1970). 'Doubling of the oscillation period with C-bifurcations in piecewise continuous systems'. *Journal of Applied Mathematics and Mechanics (Prikladnaya Matematika i Mechanika)* **34**:861–869.

M. I. Feigin (1974). 'On the generation of sets of subharmonic modes in a piecewise continuous system'. *Journal of Applied Mathematics and Mechanics (Prikladnaya Matematika i Mechanika)* **38**:810–818.

M. I. Feigin (1978). 'On the structure of C-bifurcation boundaries of piecewise continuous systems'. *Journal of Applied Mathematics and Mechanics (Prikladnaya Matematika i Mechanika)* **42**:820–829.

M. I. Feigin (1994). *Forced Oscillations in systems with discontinuous nonlinearities*. Nauka, Moscow. In Russian.

M. I. Feigin (1995). 'The increasingly complex structure of the bifurcation tree of a piecewise-smooth system'. *Journal of Applied Mathematics and Mechanics* **59**:853–863.

A. F. Filippov (1988). *Differential Equations with Discontinuous Righthand Sides*. Kluwer Academic Publishers, Dortrecht.

E. Fossas & G. Olivar (1996). 'Study of Chaos in the Buck Converter'. *IEEE Transactions on Circuits and Systems - I: Fundamental Theory and Applications* **43**:13–25.

M. H. Fredriksson & A. B. Nordmark (2000). 'On normal form calculations in impact oscillators'. *Proceedings of the Royal Society London A* **456**:315–329.

U. Galvanetto (1997). 'Bifurcations and chaos in a four-dimensional mechanical system with dry-friction'. *Journal of Sound and Vibration* **204**(4):690–695.

F. Giannakopoulos & K. Pliete (2001). 'Planar systems of piecewise linear differential equations with a line of discontinuity'. *Nonlinearity* **14**:1–22.

N. Gubar' (1971). 'Bifurcations in the vicinity of a "fused focus"'. *J. Appl. Math. Mech.* **35**:890–895.

J. Guckenheimer & P. Holmes (1983). *Nonlinear oscillations, dynamical systems and bifurcations of vector fields*. Springer.

P. Kowalczyk (2005). 'Robust chaos and border-collision bifurcations in non-invertible piecewise linear maps'. *Nonlinearity* (18):485–504.

P. Kowalczyk & M. di Bernardo (2001a). 'Existence of stable asymmetric limit cycles and chaos in unforced symmetric relay feedback systems'. In *Proceedings of European Control Conference, Porto*, pp. 1999–2004.

P. Kowalczyk & M. di Bernardo (2001b). 'On a novel class of bifurcations in hybrid dynamical systems - the case of relay feedback systems'. In *Proceedings of Hybrid Systems Computation and Control*, pp. 361–374. Springer–Verlag.

P. Kowalczyk & M. di Bernardo (2004). 'Two–parameter Degenerate Sliding Bifurcations in Filippov Systems'. submitted for journal publication.

M. Kunze (2000). *Non-Smooth Dynamical Systems, Lecture Notes in Mathematics 1744*. Springer-Verlag, Berlin.

Y. A. Kuznetsov (2004). *Elements of Applied Bifurcation Theory*. Springer-Verlag, third edn.

Y. A. Kuznetsov, et al. (2002). 'One parameter bifurcations in planar Filippov systems'. *Int. J. Bifurcation & Chaos* .

Yu.A. Kuznetsov & V.V. Levitin (1995-1997). 'CONTENT: A multiplatform environment for analyzing dynamical systems'. `ftp://ftp.cwi.nl/pub/CONTENT`.

R. Leine (2000). *Bifurcations in Discontinuous Mechanical Systems of Filippov-Type*. Ph.D. thesis, Teknische Universiteit Eindhoven, The Netherlands.

A. B. Nordmark (1991). 'Non-periodic motion caused by grazing incidence in impact oscillators'. *Journal of Sound and Vibration* **2**:279–297.

A. B. Nordmark (2002). 'Discontinuity mappings for vector fields with higher-order continuity'. Manuscript in preparation: Personal communication.

H. E. Nusse, et al. (1994). 'Border collision bifurcation: an explanation for observed bifurcation phenomena'. *Physical Review E* **49**:1073–1076.

H. E. Nusse & J. A. Yorke (1992). 'Border-collision bifurcations including 'period two to period three' for piecewise smooth systems'. *Physica D* **57**:39–57.

S. Parui & S. Banerjee (2002). 'Border collision bifurcations at the change of state-space dimension'. *CHAOS* **12**:1054–1069.

E. Pavlovskaia & M. Wiercigroch (2003). 'Modelling of vibro-impact system driven by beat frequency'. *Int. J. Mech. Sci.* **45**:623–641.

F. Peterka (1974a). 'Part 1: Theoretical analysis of n-multiple $(1/n)$-impact solutions'. *CSAV Acta Technica* **19**:462–473.

F. Peterka (1974b). 'Results of analogue computer modelling of the motion. Part 2'. *CSAV Acta Technica* **19**:569–580.

F. Peterka (1992). 'Transition to chaotic motion in mechanical systems with impacts'. *J. Sound and Vibration* **154**:95–115.

P. Piiroinen (2002). *Recurrent Dynamics of Nonsmooth Systems with Applications to Human Gait*. Ph.D. thesis, Royal Instituite of Technology, Sweden.

P. T. Piiroinen (2005). 'Numerical detection and continuation of Sliding Bifurcations in Filippov Systems Using an Event-Driven Simulator'. In preparation.

P. T. Piiroinen & Y. A. Kuznetsov (2005). 'An event driven method to simulate Filippov systems with accurate computing of sliding motions'. In preparation.

K. Popp & P. Shelter (1990). 'Stick–slip vibrations and chaos'. *Philosophical Transactions of the Royal Society A* **332**(1624):89–105.

S. W. Shaw & P. J. Holmes (1983). 'A periodically forced piecewise linear oscillator.'. *J. Sound and Vibration* **90**:129–144.

SICONOS (2005). 'http://www.enm.bris.ac.uk/staff/ptp/SICONOS_WP4/'.

D. Stewart (2000). 'Rigid-body dynamics with friction and impacts'. *SIAM Review* **42**:3–39.

J. Thompson, et al. (1983). 'Subharmonic responses and chaotic motions of a bilinear oscillator'. *IMA J. Appl. Math.* **31**:207–234.

V. I. Utkin (1992). *Sliding Modes in Control Optimization*. Springer-Verlag, Berlin.

A. J. Van der Schaft & J. M. Schumacher (2000). *An introduction to Hybrid Dynamical Systems*. Springer - Verlag.

S. Wiggins (1990). *Introduction to Applied Nonlinear Dynamical Systems and Chaos*. Springer-Verlag New York, Berlin, Heidelberg.

Y. Yoshitake & A. Sueoka (2000). *Applied nonlinear dynamics and chaos of mechanical systems with discontinuities*, chap. Forced Self-Excited Vibration with Dry Friction, pp. 237–259. World Scientific.

G. Yuan, et al. (1998). 'Border-collision bifurcations in the buck converter'. *IEEE Transactions on Circuits and Systems–I* **45**:707–716.

X. Zhao & H. Dankowicz (2004). 'Near-grazing dynamics in impact microactuators'. submitted to Nonlinearity.

Z. Zhusubaliyev & E. Mosekilde (2003). *Bifurcations and chaos in piecewise-smooth dynamical systems*. World Scientific, Singapore.

Z. T. Zhusubaliyev, et al. (2001). 'Bifurcations and chaotic oscillations in an automatic control relay system with hysteresis'. *International Journal of Bifurcations and chaos* **11**(5):1193–1231.